Optimal Beamforming Designs for Wireless Information and Power Transfer in MISO Interference Channels

Hoon Lee, *Student Member, IEEE*, Sang-Rim Lee, *Student Member, IEEE*, Kyoung-Jae Lee, *Member, IEEE*, Han-Bae Kong, *Member, IEEE*, and Inkyu Lee, *Senior Member, IEEE*

***Abstract*—This paper investigates the optimal transmit beamforming designs for simultaneous wireless information and power transfer (SWIPT) in multiple-input single-output interference channels (IFC). Based on cooperation level among transmitters and receivsers, we classify the SWIPT IFC systems into two categories. First, we consider the IFC with *partial cooperation*, where only channel state information (CSI) is available at transmitters and receivers, but not the signal waveform. Second, we examine the IFC with *signal cooperation*, where both the CSI and the signal waveforms are known to transmitters and receivers. Then, for the both scenarios, we identify the Pareto boundary of the achievable rate-energy (R-E) region which characterizes the optimal tradeoff between the information rate and the harvested energy. To this end, the problems for maximizing the information rate are formulated with minimum required harvested energy constraint. To solve these non-convex problems, we introduce parameterization techniques for characterizing the R-E region. As a result, the original problem is separated into two subproblems, for which closed-form solutions are obtained by addressing the line search method. Finally, we provide numerical examples for the Pareto boundary of the R-E region through simulations.**

***Index Terms*—Simultaneous wireless information and power transfer (SWIPT), rate-energy region, multiple antenna techniques.**

I. Introduction

In recent years, energy harvesting (EH) communication systems, where communication nodes harvest renewable energy from nature such as solar or wind, have attracted great attentions owing to its capability for supplying additional power to conventional energy-constrained systems [1]–[4]. However, scavenging energy from nature may not be practical in some situations, for instance, when there are no energy sources around the energy-demanding devices. In addition, for small wireless devices such as sensor nodes or mobile phones, it would be difficult to implement EH circuitries which gather energy from solar or wind because of limited spaces.

To overcome these issues, radio-frequency (RF) signals have been considered as a new energy source for wireless devices [5], [6]. In EH systems relying on the RF signals, a transmitter sends the RF signals to energy-demanding devices, and the energy of the RF signals can be harvested at the device. In contrast to other EH systems, such RF signal based EH techniques enable to charge energy-demanding devices whenever it is necessary. Recent experimental works have verified the feasibility of the RF signal based EH systems (please see [7] and references therein).

In conventional wireless communication systems, the role of the RF signals has been limited to conveying information, although the RF signal can carry both information and energy concurrently. Recently, exploiting the nature of the RF signals, simultaneous wireless information and power transfer (SWIPT) methods have been introduced for various system configurations. In [8], the capacity-energy function was investigated for single-input single-output (SISO) point-to-point communication systems. The results in [8] were extended to frequency-selective channels [9], and the non-trivial rate-energy (R-E) tradeoff in the SWIPT system was studied through frequency domain power allocation. The authors in [10] identified the optimal R-E tradeoff curve in two-user multiple-input multiple-output (MIMO) broadcast channels (BC). Also, for multi-user multiple-input single-output (MISO) BC systems, the weighted sum harvested energy was maximized under signal-to-noise-plus-interference ratio (SINR) constraint in [11], and transmission schemes for maximizing the secrecy rate was presented in [12]. In [13] and [14], the SWIPT relay networks were considered.

According to the cooperation level among transmitters and the receivers in interference channels (IFC), the SWIPT systems can be classified into the following two categories: IFC with *partial cooperation* (IFC-PC) [15]–[17] and with *signal cooperation* (IFC-SC) [18]. In the IFC-PC, it is assumed that only channel state information (CSI) is available at transmitters

Manuscript received August 2, 2014; revised December 16, 2014 and February 11, 2015; accepted April 22, 2015. Date of publication April 28, 2015; date of current version September 7, 2015. This work was supported in part by the National Research Foundation of Korea (NRF) funded by the Korea Government (MSIP) under Grant 2014R1A2A1A10049769 and by the Ministry of Science, ICT and Future Planning, Korea, under Grant IITP-2015-H8601-15-1006 of the Convergence Information Technology Research Center program supervised by the Institute for Information and Communications Technology Promotion. The work of K.-J Lee was supported by Basic Science Research Program through the NRF funded by the Ministry of Science, ICT and Future Planning (NRF-2013R1A1A1060503). The associate editor coordinating the review of this paper and approving it for publication was H.-C. Wu.

H. Lee, H.-B. Kong, and I. Lee are with the School of Electrical Engineering, Korea University, Seoul 136-701, Korea (e-mail: ihun1@korea.ac.kr; kongbae@korea.ac.kr; inkyu@korea.ac.kr).

S.-R. Lee is with the Advanced Standard Research and Development Laboratory, LG Electronics, Seoul 137-130, Korea (e-mail: sangrim78@korea.ac.kr).

K.-J. Lee is with the Department of Electronics and Control Engineering, Hanbat National University, Daejeon 305-719, Korea (e-mail: kyoungjae@hanbat.ac.kr).

Color versions of one or more of the figures in this paper are available online at http://ieeexplore.ieee.org.

Digital Object Identifier 10.1109/TWC.2015.2427168

and receivers, but not the transmitted signal. On the other hand, in the IFC-SC systems, both the CSI and the signal waveforms are known at the transmitters and the receivers since the energy-carrying RF signal can be determined in advance. Then, we can improve the achievable R-E performance by constructing the transmitted signals as a superposition of the information signal and the energy signal components [11], [18]. Also, with the pre-determined energy signal, the receivers can eliminate the interference induced by the energy signal to improve data rate. Therefore, the capability of SWIPT is significantly improved in the IFC-SC at the expense of increased complexity for the additional signal processing and the non-linear receiver structure for the interference cancellation. In a two-user MIMO IFC-PC, [15] found a necessary condition for the optimal transmission strategy in high signal-to-noise ratio regime. Based on this necessary condition, practical SWIPT transmission schemes and their achievable R-E regions were investigated in [15], and were extended to a general K-user MIMO IFC-PC [16]. The weighted sum rate maximizing algorithms were provided in [17] for the MISO IFC-PC, but the achievable R-E region was not analyzed. Recently, the authors in [18] introduced the collaborative signal transmission and interference cancelling protocols for the general K-user SISO IFC-SC.

In this paper, we design the optimal linear beamforming vectors for the SWIPT systems in two-user MISO IFC-PC and IFC-SC, where each of two transmitters sends data or transfers energy to its corresponding receiver. Since it is not easy to simultaneously decode information and harvest energy at the receiver due to implementation issues in practical systems [10], [11], [15], we assume that receivers behave as either an information decoding (ID) receiver or an EH receiver, but not as both at the same time.

Then, in the two-user IFC, there exist three different scenarios depending on the receivers' mode [15]. First, when there are two ID receivers, the system is equivalent to a conventional IFC, and thus existing methods for the IFC in [19]–[25] can be applied. Second, for the case of two EH receivers, we can easily find the optimal beamforming vectors which maximize the total harvested energy at the EH receivers [15]. Third, if there are one ID receiver and one EH receiver, it is not easy to design the beamforming vectors which optimize both the information rate and the harvested energy, since there exists a non-trivial tradeoff between two quantities. In this paper, we focus on this case, and investigate the optimal tradeoff between the information rate and the harvested energy by characterizing the Pareto boundary of the achievable R-E region.

For both the IFC-PC and the IFC-SC systems, we formulate the information rate maximization problems under minimum required harvested energy constraints to obtain the Pareto boundary. As these are non-convex optimization problems, it is difficult to obtain the globally optimal solution. To solve this issue, we introduce new parameters, namely *energy splitting* and *power splitting* parameters, for the IFC-PC and the IFC-SC, respectively. The energy splitting parameter in the IFC-PC divides the harvested energy constraint of the EH receiver into two parts, and adjusts the amount of energy conveyed from each transmitters. For the IFC-SC, the power splitting parameter splits the transmit power constraints at transmitters,

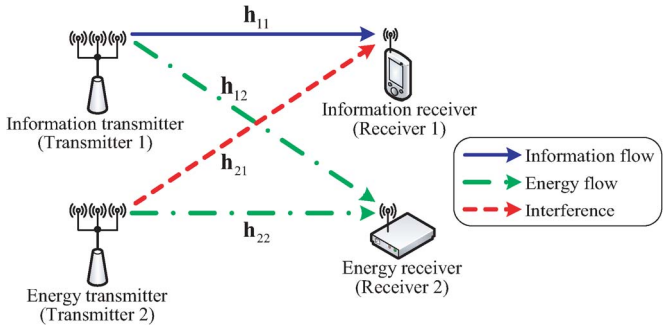

Fig. 1. Schematic diagram for the SWIPT system in two-user MISO IFC.

and enables the signaling cooperative transmission. By utilizing these parameters, the original non-convex problems can be separated into two connected subproblems in both of the IFC-PC and the IFC-SC cases.

The first subproblem designs beamforming vectors, whereas the second one finds the optimal parameter by a simple line search method. Still, the first problem is a non-convex quadratically constrained quadratic program (QCQP), and it is difficult to determine the globally optimal solution. Thus, we apply the semi-definite relaxation (SDR) method to the non-convex QCQP, and the optimal solution achieving the Pareto boundary is obtained with a closed-form. Then, we present numerical examples for the achievable R-E region and attain some insightful results on the optimal transmission schemes.

This paper is organized as follows: In Section II, we introduce the system model and formulate the problem for two-user MISO IFC-PC and IFC-SC. Section III characterizes the achievable R-E region of the IFC-PC by utilizing the energy splitting parameter, and Section IV provides the optimal beamforming designs achieving the Pareto boundary. For the IFC-SC, the optimal transmission strategy is provided in Section V. In Section VI, we observe insightful results on the Pareto boundary through numerical simulations. Finally, the paper is terminated with conclusions in Section VII.

Throughout this paper, we employ uppercase boldface letters, lowercase boldface letters, and normal letters for matrices, vectors, and scalar quantities, respectively. A set of all complex matrices of size m-by-n is denoted by $\mathbb{C}^{m\times n}$, and conjugate transpose of a matrix or a vector is represented by $(\cdot)^H$. In addition, $\mathrm{tr}(\mathbf{X})$ and $\mathrm{rank}(\mathbf{X})$ stand for trace and rank of a matrix $\mathbf{X}$, respectively. $\mathbf{I}_m$ accounts for an identity matrix of size m-by-m. The absolute value of a scalar is given by $|\cdot|$, and $\|\cdot\|$ indicates the 2-norm operation of a vector. Also, the matrix $\mathbf{\Pi}_{\mathbf{x}}^{\perp} = \mathbf{I}_m - \mathbf{x}\mathbf{x}^H/\|\mathbf{x}\|^2$ denotes the projection matrix onto the nullspace of a vector $\mathbf{x} \in \mathbb{C}^{m\times 1}$

II. System Model

In this section, we provide a system model for two-user MISO IFC for the SWIPT system where two transmitters each equipped with M antennas transmit the RF signals to single antenna receivers as shown in Fig. 1. First, a system model for the IFC-PC is explained, and then it is followed by the description of the IFC-SC system.

A. IFC-PC

In the IFC-PC system, we assume that only the perfect CSI is available at the transmitters and the receivers, but not the transmitted symbols. In this configuration, the ID receiver decodes data conveyed from the information transmitter, while the EH receiver harvests energy[1] of the RF signals transferred from both the energy and information transmitters. Then, the RF signal transmitted from the energy transmitter to the ID receiver acts as interference, whereas the information transmitter helps the EH receiver collect more energy.

For notational conveniences, we denote the information and the energy transmitter as transmitter 1 and 2, respectively, and the ID and the EH receiver as receiver 1 and 2, respectively. Assuming frequency-flat fading, the channel vector from transmitter i to receiver j is expressed as $\mathbf{h}_{ij} \in \mathbb{C}^{M\times 1}$ for $i, j = 1, 2$. Also, we denote s_i as the scalar symbol transmitted from transmitter i with $s_i \sim \mathcal{CN}(0, 1)$[2] $(i = 1, 2)$, and it is assumed that s_1 and s_2 are independent. Note that s_1 is an information symbol bearing the data of the ID receiver, while an energy symbol s_2 carries energy to the EH receiver but not any information.

Then, the received signal at receiver i $(i = 1, 2)$ is given by

$$y_i = \mathbf{h}_{ii}^H \mathbf{w}_i s_i + \mathbf{h}_{\bar{i}i}^H \mathbf{w}_{\bar{i}} s_{\bar{i}} + n_i,$$

where we define $\bar{i} = 1$ for $i = 2$ and $\bar{i} = 2$ for $i = 1$, $\mathbf{w}_i \in \mathbb{C}^{M\times 1}$ represents the linear beamforming vector at transmitter i with transmit power constraint $\|\mathbf{w}_i\|^2 \le P_i$, and n_i indicates the complex Gaussian noise at receiver i with zero mean and unit variance.

In the IFC-PC, it is assumed that the ID receiver cannot perform interference cancelation, and thus the energy signal interference is treated as an additive noise [12], [15], [16]. Then, the achievable information rate at the ID receiver is written by

$$R_{\text{IFC-PC}} = \log_2\left(1 + \frac{\left|\mathbf{h}_{11}^H \mathbf{w}_1\right|^2}{1 + \left|\mathbf{h}_{21}^H \mathbf{w}_2\right|^2}\right).$$

On the other hand, the EH receiver can harvest energy using the RF signals transferred from both transmitters. Therefore, the harvested energy at the EH receiver can be obtained as

$$E_{\text{IFC-PC}} = \mathbb{E}\left[|y_2|^2\right] = \left|\mathbf{h}_{22}^H \mathbf{w}_2\right|^2 + \left|\mathbf{h}_{12}^H \mathbf{w}_1\right|^2,$$

where the noise power is ignored in $E_{\text{IFC-PC}}$, since it is practically mush smaller compared to that of the signal power [10]. Then, there exists a non-trivial tradeoff between the information rate $R_{\text{IFC-PC}}$ and the harvested energy $E_{\text{IFC-PC}}$, and this is the topic which we focus on this paper.

[1]For conveniences, we normalize the time slot duration to unity, and thus the power and energy terms are interchangeably used throughout this paper.

[2]In fact, we do not need to set s_2 as Gaussian random variable since it does not carry any information. However, in the IFC-PC systems, we assume that s_2 is Gaussian for the tractable information rate expression.

To specify the tradeoff relationship between $R_{\text{IFC-PC}}$ and $E_{\text{IFC-PC}}$, let us denote the achievable R-E region for the IFC-PC system as

$$\mathcal{C}_{\text{IFC-PC}}(P_1, P_2) = \left\{(R_{\text{IFC-PC}}, E_{\text{IFC-PC}}) : R_{\text{IFC-PC}} \le \log_2\left(1 + \frac{\left|\mathbf{h}_{11}^H \mathbf{w}_1\right|^2}{1+\left|\mathbf{h}_{21}^H \mathbf{w}_2\right|^2}\right), \; E_{\text{IFC-PC}} \le \left|\mathbf{h}_{12}^H \mathbf{w}_1\right|^2 + \left|\mathbf{h}_{22}^H \mathbf{w}_2\right|^2, \|\mathbf{w}_1\|^2 \le P_1, \|\mathbf{w}_2\|^2 \le P_2\right\}.$$

The Pareto boundary is defined as a R-E point $(R, E) \in \mathcal{C}_{\text{IFC-PC}}(P_1, P_2)$ which does not have another R-E point (R', E') such that $(R', E') \ge (R, E)$ and $(R', E') \ne (R, E)$, where the inequality is componentwise [22], and this characterizes the optimal tradeoff between $R_{\text{IFC-PC}}$ and $E_{\text{IFC-PC}}$. Thus, in the following, we provide a method for obtaining all Pareto boundary points of $\mathcal{C}_{\text{IFC-PC}}(P_1, P_2)$.

By finding the maximum information rate under minimum required harvested energy constraint, a Pareto point of $\mathcal{C}_{\text{IFC-PC}}(P_1, P_2)$ can be identified, and the information rate maximization problem for given EH constraint Q is formulated by

$$R^{\star}_{\text{IFC-PC}}(Q) = \max_{\mathbf{w}_1, \mathbf{w}_2} \log_2\left(1 + \frac{\left|\mathbf{h}_{11}^H \mathbf{w}_1\right|^2}{1 + \left|\mathbf{h}_{21}^H \mathbf{w}_2\right|^2}\right) \tag{1}$$

$$s.t. \; \|\mathbf{w}_i\|^2 \le P_i, \; i = 1, 2,$$

$$\left|\mathbf{h}_{12}^H \mathbf{w}_1\right|^2 + \left|\mathbf{h}_{22}^H \mathbf{w}_2\right|^2 \ge Q, \tag{2}$$

where (2) stands for the minimum required harvested energy constraint at the EH receiver. If we solve the problem in (1) for all valid EH constraint Q, then the all Pareto boundary points $(R^{\star}_{\text{IFC-PC}}(Q), Q)$ are completely characterized. However, it is difficult to find the globally optimal solution since the problem (1) is non-convex. Also, due to the EH constraint (2), existing solutions for a conventional MISO IFC [19]–[25] cannot be applied to this configuration. Note that before we solve the problem (1), the valid region for Q should be identified. This will be addressed in Section II-C.

B. IFC-SC

In this subsection, we describe a system model for the IFC-SC scheme [18]. It is worth noting that since the energy symbol s_2 does not carry any information, we can pre-determine s_2 as an arbitrary random variable or a fixed symbol. Therefore, in addition to the perfect CSI, this pre-determined energy symbol s_2 can be known at all the transmitters and the ID receiver in advance.

At the information transmitter, we apply the signal splitting approach [11], [18] which constructs the signal vector sent from the information transmitter $\mathbf{x}_1 \in \mathbb{C}^{M\times 1}$ as a superposition of the information symbol s_1 and the energy symbol s_2. Denoting $\mathbf{g}_{1,\text{I}} \in \mathbb{C}^{M\times 1}$ and $\mathbf{g}_{1,\text{E}} \in \mathbb{C}^{M\times 1}$ as the beamforming vectors at the information transmitter for the information and the energy symbol, respectively, $\mathbf{x}_1$ is expressed as

$$\mathbf{x}_1 = \mathbf{g}_{1,\text{I}} s_1 + \mathbf{g}_{1,\text{E}} s_2.$$

Then, for the IFC-SC, the received signal r_i at receiver i ($i = 1, 2$) are written by

$$r_1 = \mathbf{h}_{11}^H \mathbf{g}_{1,\mathrm{I}} s_1 + \left(\mathbf{h}_{11}^H \mathbf{g}_{1,\mathrm{E}} + \mathbf{h}_{21}^H \mathbf{g}_2\right) s_2 + n_1, \quad (3)$$

$$r_2 = \mathbf{h}_{12}^H \mathbf{g}_{1,\mathrm{I}} s_1 + \left(\mathbf{h}_{22}^H \mathbf{g}_2 + \mathbf{h}_{12}^H \mathbf{g}_{1,\mathrm{E}}\right) s_2 + n_2, \quad (4)$$

where $\mathbf{g}_2 \in \mathbb{C}^{M\times 1}$ stands for the beamforming vector at the energy transmitter in the IFC-SC system.

With the energy symbol s_2 at hand, to improve the information rate, the ID receiver can perfectly cancel the interference caused by the energy symbol s_2, i.e., $(\mathbf{h}_{11}^H \mathbf{g}_{1,\mathrm{E}} + \mathbf{h}_{21}^H \mathbf{g}_2) s_2$ in (3). Thus, in the IFC-SC scenario, the achievable information rate at the ID receiver is obtained as

$$R_{\text{IFC-SC}} = \log_2\left(1 + \left|\mathbf{h}_{11}^H \mathbf{g}_{1,\mathrm{I}}\right|^2\right).$$

Meanwhile, the EH receiver harvests the energy of the received RF signal (4), and the harvested energy in the IFC-SC can be given by

$$E_{\text{IFC-SC}} = \mathbb{E}\left[|r_2|^2\right] = \left|\mathbf{h}_{22}^H \mathbf{g}_2 + \mathbf{h}_{12}^H \mathbf{g}_{1,\mathrm{E}}\right|^2 + \left|\mathbf{h}_{12}^H \mathbf{g}_{1,\mathrm{I}}\right|^2.$$

Similar to the IFC-PC systems, we will provide the optimal tradeoff between $R_{\text{IFC-SC}}$ and $E_{\text{IFC-SC}}$, which is characterized by the Pareto boundary of the achievable R-E region $\mathcal{C}_{\text{IFC-SC}}(P_1, P_2)$. Here, the R-E region for the IFC-SC $\mathcal{C}_{\text{IFC-SC}}(P_1, P_2)$ is defined as

$$\begin{aligned}&\mathcal{C}_{\text{IFC-SC}}(P_1, P_2)\\ &= \Big\{(R_{\text{IFC-SC}}, E_{\text{IFC-SC}}) : R_{\text{IFC-SC}} = \log_2\left(1 + \left|\mathbf{h}_{11}^H \mathbf{g}_{1,\mathrm{I}}\right|^2\right),\\ &\quad E_{\text{IFC-SC}} = \left|\mathbf{h}_{22}^H \mathbf{g}_2 + \mathbf{h}_{12}^H \mathbf{g}_{1,\mathrm{E}}\right|^2 + \left|\mathbf{h}_{12}^H \mathbf{g}_{1,\mathrm{I}}\right|^2,\\ &\quad \|\mathbf{g}_{1,\mathrm{I}}\|^2 + \|\mathbf{g}_{1,\mathrm{E}}\|^2 \le P_1, \|\mathbf{g}_2\|^2 \le P_2\Big\}.\end{aligned}$$

To find a Pareto boundary point of $\mathcal{C}_{\text{IFC-SC}}(P_1, P_2)$, we solve the following information rate maximization problem for given EH constraint U.

$$\begin{aligned}R^{\star}_{\text{IFC-SC}}(U) = \max_{\mathbf{g}_{1,\mathrm{I}}, \mathbf{g}_{1,\mathrm{E}}, \mathbf{g}_2} &\log_2\left(1 + \left|\mathbf{h}_{11}^H \mathbf{g}_{1,\mathrm{I}}\right|^2\right)\\ s.t.\ &\|\mathbf{g}_{1,\mathrm{I}}\|^2 + \|\mathbf{g}_{1,\mathrm{E}}\|^2 \le P_1,\ \|\mathbf{g}_2\|^2 \le P_2,\\ &\left|\mathbf{h}_{22}^H \mathbf{g}_2 + \mathbf{h}_{12}^H \mathbf{g}_{1,\mathrm{E}}\right|^2 + \left|\mathbf{h}_{12}^H \mathbf{g}_{1,\mathrm{I}}\right|^2 \ge U. \quad (5)\end{aligned}$$

Note that, unlike the SISO IFC-SC [18], we should optimize the beamforming vectors for both the information and the energy signals. Therefore, a solution for (5) can be viewed as a generalization of the two-user SISO IFC-SC systems with one information transmitter-receiver pair and one energy transmitter-receiver pair. Similar to the IFC-PC systems, the Pareto boundary point $(R^{\star}_{\text{IFC-SC}}(U), U) \in \mathcal{C}_{\text{IFC-SC}}(P_1, P_2)$ can be identified by solving problem (5) for valid EH constraint U, which will be given in the following subsection.

C. Valid EH Constraints Q and U

Before solving the problems in (1) and (5), in this subsection, we discuss the valid region for the EH constraints Q and U. To this end, we first compute two special R-E boundary points, namely the maximum harvested energy and the maximum information rate points, for the BC, the IFC-PC, and the IFC-SC systems. Then, the valid EH constraints Q and U will be addressed.

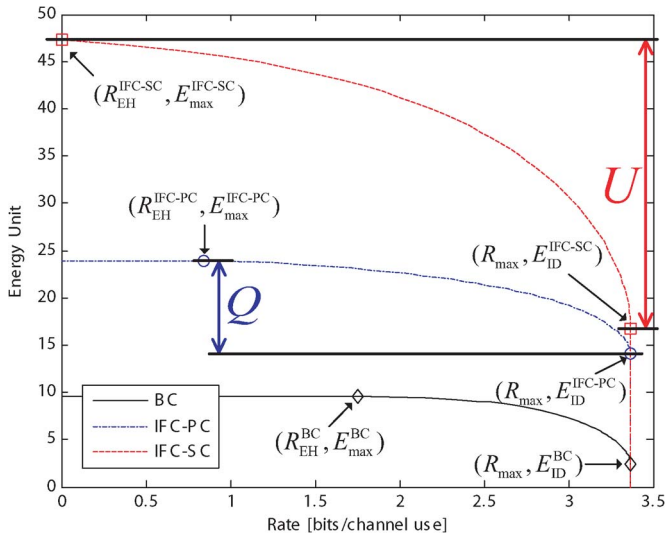

Fig. 2. Pareto boundary and valid EH constraint.

1) BC Boundary Points: Note that the BC is a special case of the IFC-PC with $\mathbf{w}_2 = \mathbf{0}$. Then, as illustrated in Fig. 2, we can define two Pareto boudnary points of the BC $(R_{\text{EH}}^{\text{BC}}, E_{\text{max}}^{\text{BC}})$ and $(R_{\text{max}}, E_{\text{ID}}^{\text{BC}})$ as [10]

$$\left(R_{\text{EH}}^{\text{BC}}, E_{\text{max}}^{\text{BC}}\right) = \left(\log_2\left(1 + P_1 \frac{\left|\mathbf{h}_{11}^H \mathbf{h}_{12}\right|^2}{\|\mathbf{h}_{12}\|^2}\right), P_1 \|\mathbf{h}_{12}\|^2\right), \quad (6)$$

$$\left(R_{\text{max}}, E_{\text{ID}}^{\text{BC}}\right) = \left(\log_2\left(1 + P_1 \|\mathbf{h}_{11}\|^2\right), P_1 \frac{\left|\mathbf{h}_{12}^H \mathbf{h}_{11}\right|^2}{\|\mathbf{h}_{11}\|^2}\right), \quad (7)$$

where the points (6) and (7) represent the maximum harvested energy and the maximum information rate point in the BC, respectively. The maximum energy point for the BC in (6) can be obtained with the beamforming vector $\mathbf{w}_1 = \sqrt{P_1}\frac{\mathbf{h}_{12}}{\|\mathbf{h}_{12}\|} \triangleq \mathbf{v}_1^{\text{EH}}$ which is aligned to the EH receiver, while the maximum rate point in (7) can be achieved via $\mathbf{w}_1 = \sqrt{P_1}\frac{\mathbf{h}_{11}}{\|\mathbf{h}_{11}\|} \triangleq \mathbf{v}_1^{\text{ID}}$ which is aligned to the ID receiver.

2) IFC-PC Boundary Points: As shown in Fig. 2, there exist two special Pareto points $(R_{\text{EH}}^{\text{IFC-PC}}, E_{\text{max}}^{\text{IFC-PC}})$ and $(R_{\text{max}}, E_{\text{ID}}^{\text{IFC-PC}})$ in the IFC-PC. The maximum energy point of the IFC-PC $(R_{\text{EH}}^{\text{IFC-PC}}, E_{\text{max}}^{\text{IFC-PC}})$ is calculated as

$$\begin{aligned}&\left(R_{\text{EH}}^{\text{IFC-PC}}, E_{\text{max}}^{\text{IFC-PC}}\right)\\ &= \left(\log_2\left(1 + \frac{P_1 \left|\mathbf{h}_{11}^H \mathbf{h}_{12}\right|^2 / \|\mathbf{h}_{12}\|^2}{1 + P_2 \left|\mathbf{h}_{21}^H \mathbf{h}_{22}\right|^2 / \|\mathbf{h}_{22}\|^2}\right), E_{\text{max}}^{\text{BC}} + P_2 \|\mathbf{h}_{22}\|^2\right).\end{aligned}$$

It is easy to show that this point is computed with the beamforming vectors $\mathbf{w}_1 = \mathbf{v}_1^{\text{EH}}$ and $\mathbf{w}_2 = \sqrt{P_2}\frac{\mathbf{h}_{22}}{\|\mathbf{h}_{22}\|} \triangleq \mathbf{v}_2^{\text{EH}}$, i.e., both the beamforming vectors are aligned to the EH receiver.

On the other hand, to achieve the maximum information rate point $(R_{\text{max}}, E_{\text{ID}}^{\text{IFC-PC}})$, the information transmitter applies the beamforming vector $\mathbf{w}_1 = \mathbf{v}_1^{\text{ID}}$, while the zero forcing (ZF) beamforming vector $\mathbf{w}_2 = \sqrt{P_2}\frac{\mathbf{\Pi}_{\mathbf{h}_{21}}^{\perp}\mathbf{h}_{22}}{\|\mathbf{\Pi}_{\mathbf{h}_{21}}^{\perp}\mathbf{h}_{22}\|}$ is utilized at the energy transmitter not to interfere the ID receiver. As a result, the corresponding energy point $E_{\text{ID}}^{\text{IFC-PC}}$ is obtained as $E_{\text{ID}}^{\text{IFC-PC}} = E_{\text{ID}}^{\text{BC}} + E_{\text{ZF}}$, where $E_{\text{ZF}} = P_2 \|\mathbf{\Pi}_{\mathbf{h}_{21}}^{\perp}\mathbf{h}_{22}\|^2$ indicates the energy transferred from the energy transmitter to the EH receiver with

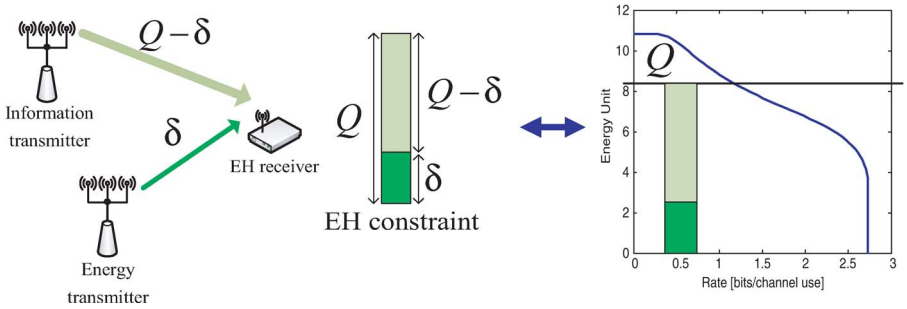

Fig. 3. Graphical interpretation of the energy splitting parameter δ in the IFC-PC system.

the ZF beamforming vector. From Fig. 2, we can observe that the Pareto boundary points of the R-E region $\mathcal{C}_{\text{IFC-PC}}(P_1, P_2)$ are corresponding to the boundary points (R, E) for $R_{\text{EH}}^{\text{IFC-PC}} \leq R \leq R_{\max}$ and $E_{\text{ID}}^{\text{IFC-PC}} \leq E \leq E_{\max}^{\text{IFC-PC}}$. Therefore, by solving problem (1) for $E_{\text{ID}}^{\text{IFC-PC}} \leq Q \leq E_{\max}^{\text{IFC-PC}}$, all Pareto boundary points for the IFC-PC can be identified.

3) IFC-SC Boundary Points: Similar to the IFC-PC case, two special Pareto points $(R_{\text{EH}}^{\text{IFC-SC}}, E_{\max}^{\text{IFC-SC}})$ and $(R_{\max}^{\text{IFC-SC}}, E_{\text{ID}}^{\text{IFC-SC}})$ can be computed as

$$\left(R_{\text{EH}}^{\text{IFC-SC}}, E_{\max}^{\text{IFC-SC}}\right) = \left(0, \left(\sqrt{E_{\max}^{\text{BC}}} + \sqrt{P_2}\|\mathbf{h}_{22}\|\right)^2\right), \tag{8}$$

$$\left(R_{\max}, E_{\text{ID}}^{\text{IFC-SC}}\right) = \left(\log_2\left(1+P_1\|\mathbf{h}_{11}\|^2\right), E_{\text{ID}}^{\text{BC}} + P_2\|\mathbf{h}_{22}\|^2\right). \tag{9}$$

Here, the maximum harvested energy point (8) in the IFC-SC is achieved with $\mathbf{g}_{1,\text{I}} = \mathbf{0}$, $\mathbf{g}_{1,\text{E}} = \mathbf{v}_1^{\text{EH}}$, and $\mathbf{g}_2 = \mathbf{v}_2^{\text{EH}}$, while the maximum information rate point (9) is attained by applying $\mathbf{g}_{1,\text{I}} = \mathbf{v}_1^{\text{ID}}$, $\mathbf{g}_{1,\text{E}} = \mathbf{0}$, and $\mathbf{g}_2 = \mathbf{v}_2^{\text{EH}}$. Thus, as illustrated in Fig. 2, we set the EH constraint in the IFC-SC problem (5) as $E_{\text{ID}}^{\text{IFC-SC}} \leq U \leq E_{\max}^{\text{IFC-SC}}$. Now, we can identify the Pareto boundary for the IFC-PC and the IFC-SC with the valid Q and U, respectively. We first investigate the optimal beamforming designs for the IFC-PC in Sections III and IV, and then address the IFC-SC in Section V.

III. Characterization of the Pareto Boundary For the IFC-PC

In this section, we provide an approach to obtain the Pareto boundary of the R-E region for the IFC-PC $\mathcal{C}_{\text{IFC-PC}}(P_1, P_2)$ by reformulating the original non-convex problem in (1) into two sequential subproblems. To this end, we introduce the energy splitting parameter δ, which represents the amount of energy transferred from the energy transmitter to the EH receiver as illustrated in Fig. 3. For satisfying the EH constraint Q, the energy transmitter sends the energy δ, while the information transmitter provides the energy $Q - \delta$ to the EH receiver. The details are presented in the following theorem.

Theorem 1: The optimal information rate $R_{\text{IFC-PC}}^{\star}(Q)$ in the original problem (1) is the same as that in the following maximization problem:

$$\Upsilon(Q) = \max_{\delta} \tilde{R}_{\text{IFC-PC}}(\delta, Q) \tag{10}$$

$$s.t.\ \delta_{\min} \leq \delta \leq \delta_{\max}, \tag{11}$$

where $\delta_{\min} = (Q - E_{\max}^{\text{BC}})^+$ and $\delta_{\max} = \min\{Q, P_2\|\mathbf{h}_{22}\|^2\}$ with $(x)^+ = \max\{0, x\}$. Here, $\tilde{R}_{\text{IFC-PC}}(\delta, Q)$ is defined as

$$\tilde{R}_{\text{IFC-PC}}(\delta, Q) = \max_{\mathbf{w}_1, \mathbf{w}_2} \log_2\left(1 + \frac{\left|\mathbf{h}_{11}^H \mathbf{w}_1\right|^2}{1 + \left|\mathbf{h}_{21}^H \mathbf{w}_2\right|^2}\right) \tag{12}$$

$$s.t.\ \|\mathbf{w}_i\|^2 \leq P_i,\ i = 1, 2,$$

$$\left|\mathbf{h}_{12}^H \mathbf{w}_1\right|^2 \geq Q - \delta, \tag{13}$$

$$\left|\mathbf{h}_{22}^H \mathbf{w}_2\right|^2 \geq \delta. \tag{14}$$

Proof: We first show that the feasible range of the energy splitting parameter δ is given by (11). From (13) and (14), δ is bounded by

$$Q - \left|\mathbf{h}_{12}^H \mathbf{w}_1\right|^2 \leq \delta \leq \left|\mathbf{h}_{22}^H \mathbf{w}_2\right|^2. \tag{15}$$

Denoting the feasible set of the problem (12) as

$$\tilde{\mathcal{W}}(\delta, Q, P_1, P_2) = \Big\{(\mathbf{w}_1, \mathbf{w}_2) : \left|\mathbf{h}_{12}^H \mathbf{w}_1\right|^2 \geq Q - \delta, \left|\mathbf{h}_{22}^H \mathbf{w}_2\right|^2 \geq \delta, \|\mathbf{w}_i\|^2 \leq P_i,\ \forall i = 1, 2\Big\},$$

the condition (15) should be satisfied for any $(\mathbf{w}_1, \mathbf{w}_2) \in \tilde{\mathcal{W}}(\delta, \bar{E}, P_1, P_2)$.

Thus, we have

$$\delta \geq Q - \max_{\mathbf{w}_1} \left|\mathbf{h}_{12}^H \mathbf{w}_1\right|^2 = Q - P_1\|\mathbf{h}_{12}\|^2, \tag{16}$$

$$\delta \leq \max_{\mathbf{w}_2} \left|\mathbf{h}_{22}^H \mathbf{w}_2\right|^2 = P_2\|\mathbf{h}_{22}\|^2. \tag{17}$$

Since δ stands for the energy transferred from the energy transmitter, δ is basically bounded by $0 \leq \delta \leq Q$. Combining this with (16) and (17), the feasible range of δ is obtained as (11).

Now, we prove that the optimal rate $R_{\text{IFC-PC}}^{\star}(Q)$ in the original problem (1) equals $\Upsilon(Q)$ in (10), which indicates the optimal value of the problem in (12). Let us define the feasible set of the original problem in (1) as

$$\mathcal{W}(Q, P_1, P_2) = \Big\{(\mathbf{w}_1, \mathbf{w}_2) : \left|\mathbf{h}_{12}^H \mathbf{w}_1\right|^2 + \left|\mathbf{h}_{22}^H \mathbf{w}_2\right|^2 \geq Q, \|\mathbf{w}_i\|^2 \leq P_i,\ \forall i = 1, 2\Big\}. \tag{18}$$

It is worth noting that $\tilde{\mathcal{W}}(\delta, Q, P_1, P_2) \subseteq \mathcal{W}(Q, P_1, P_2)$ must be true for any feasible δ, since any pair of beamforming vectors $(\mathbf{w}_1, \mathbf{w}_2)$ on both constraints (13) and (14) always satisfies the EH constraint (2), but not vice versa.

Using this fact, we will first show that $R_{\text{IFC-PC}}^{\star}(Q) \leq \Upsilon(Q)$. Defining $\mathbf{w}_1^{\star}$ and $\mathbf{w}_2^{\star}$ as the optimal solution for the original problem (1), we can always find at least one $\hat{\delta}$ such

that $(\mathbf{w}_1^\star, \mathbf{w}_2^\star) \in \tilde{\mathcal{W}}(\hat{\delta}, Q, P_1, P_2)$, for example, by setting $\hat{\delta} = |\mathbf{h}_{22}^H \mathbf{w}_2^\star|^2$. Then, the optimal solution of the problem in (12) with $\delta = \hat{\delta}$ must be $(\mathbf{w}_1^\star, \mathbf{w}_2^\star)$ since $\tilde{\mathcal{W}}(\hat{\delta}, Q, P_1, P_2) \subseteq \mathcal{W}(Q, P_1, P_2)$. Therefore, it follows:

$$R^\star_{\text{IFC-PC}}(Q) = \tilde{R}_{\text{IFC-PC}}(\hat{\delta}, Q) \le \max_{\delta} \tilde{R}_{\text{IFC-PC}}(\delta, Q) = \Upsilon(Q). \quad (19)$$

Next, to verify that $R^\star_{\text{IFC-PC}}(Q) \ge \Upsilon(Q)$, we represent $(\tilde{\boldsymbol{w}}_1(\delta), \tilde{\boldsymbol{w}}_2(\delta))$ as a pair of the optimal beamforming vector for the problem (12) with a given δ. Denoting $\delta^\star$ as the optimal solution for (10), we have $\tilde{\mathcal{W}}(\delta^\star, Q, P_1, P_2) \subseteq \mathcal{W}(Q, P_1, P_2)$, which means that the feasible region of the original problem (1) always contains $(\tilde{\boldsymbol{w}}_1(\delta^\star), \tilde{\boldsymbol{w}}_2(\delta^\star))$. Then $\Upsilon(Q)$ is bounded by

$$R^\star_{\text{IFC-PC}}(Q) \ge \tilde{R}_{\text{IFC-PC}}(\delta^\star, Q) = \Upsilon(Q). \quad (20)$$

By combining (19) and (20), we conclude $R^\star_{\text{IFC-PC}}(Q) = \Upsilon(Q)$. This completes the proof. ■

Theorem 1 implies that the optimal information rate $R^\star_{\text{IFC-PC}}(Q)$ for a given EH constraint Q, which is originally found by solving (1), can be equivalently obtained from (10) and (12). In other words, the Pareto boundary point $(R^\star_{\text{IFC-PC}}(Q), Q)$ of $\mathcal{C}_{\text{IFC-PC}}(P_1, P_2)$ can be computed by performing the following two step approach: First, we identify $\tilde{R}_{\text{IFC-PC}}(\delta, Q)$ for all feasible δ, and then $R^\star_{\text{IFC-PC}}(Q)$ is determined via one-dimensional line search over $\delta_{\min} \le \delta \le \delta_{\max}$. In Section IV, we will show that the optimal energy splitting parameter $\delta^\star$ can be computed by the bisection method [26] without loss of optimality.

IV. Optimal Beamforming Vector Design for the IFC-PC

In this section, we provide methods for designing the optimal beamforming vectors which attain the Pareto boundary points of the achievable R-E region for the IFC-PC. As discussed in Section III, we first obtain the optimal solutions $\tilde{\mathbf{w}}_1(\delta)$ and $\tilde{\mathbf{w}}_2(\delta)$ in the problem (12) for a given δ, and then present the algorithm to identify the optimal energy splitting parameter $\delta^\star$ in the problem (10).

A. Optimal Beamforming Vectors

Since the EH constraints (13) and (14) depend only on the one variable, the problem (12) is fully separated into the following two subproblems:

$$I(\delta) = \min_{\mathbf{w}_2} \left|\mathbf{h}_{21}^H \mathbf{w}_2\right|^2 \quad s.t.\ \|\mathbf{w}_2\|^2 \le P_2,\ \left|\mathbf{h}_{22}^H \mathbf{w}_2\right|^2 \ge \delta, \quad (21)$$

and

$$\tilde{R}_{\text{IFC-PC}}(\delta, Q) = \max_{\mathbf{w}_1} \log_2\left(1 + \frac{\left|\mathbf{h}_{11}^H \mathbf{w}_1\right|^2}{1 + I(\delta)}\right) \quad s.t.\ \|\mathbf{w}_1\|^2 \le P_1,\ \left|\mathbf{h}_{12}^H \mathbf{w}_1\right|^2 \ge Q - \delta, \quad (22)$$

where $I(\delta)$ represents the interference power at the ID receiver induced by the energy transmitter.

Since $I(\delta)$ does not affect the optimal solution for (22), the problem (22) becomes the rate maximization problem for the MISO BC under EH constraint $Q - \delta$, whose closed-form solution is given as [10]

$$\tilde{\mathbf{w}}_1(\delta) = \begin{cases} \sqrt{\frac{Q-\delta}{\|\mathbf{h}_{12}\|^2}}\alpha \frac{\mathbf{h}_{12}}{\|\mathbf{h}_{12}\|} \\ \quad + \sqrt{P_1 - \frac{Q-\delta}{\|\mathbf{h}_{12}\|^2}} \frac{\boldsymbol{\Pi}^\perp_{\mathbf{h}_{12}} \mathbf{h}_{11}}{\left\|\boldsymbol{\Pi}^\perp_{\mathbf{h}_{12}} \mathbf{h}_{11}\right\|}, & \text{for } \delta_{\min} \le \delta < \delta_1, \\ \sqrt{P_1} \frac{\mathbf{h}_{11}}{\|\mathbf{h}_{11}\|}, & \text{for } \delta_1 \le \delta \le \delta_{\max}, \end{cases}$$

where the complex number α is defined as $\alpha = \mathbf{h}_{12}^H \mathbf{h}_{11} / |\mathbf{h}_{12}^H \mathbf{h}_{11}|$. Here, the threshold δ_1 determines the formula for $\tilde{\mathbf{w}}_1(\delta)$, and can be written as $\delta_1 = \min\{Q - E_{\text{ID}}^{\text{BC}}, P_2 \|\mathbf{h}_{22}\|^2\}$. Note that the threshold δ_1 is different from the BC case [10] due to the parameter δ.[3]

Now, the remaining work is to solve (21), which is a non-convex QCQP, and thus it is still hard to find the globally optimal solution. To address the problem efficiently, we employ the SDR techniques which obtain an approximate solution for the non-convex QCQP. Defining the transmit covariance matrix of the energy transmitter as $\mathbf{S}_2 = \mathbf{w}_2 \mathbf{w}_2^H$ and ignoring the rank constraint $\text{rank}(\mathbf{S}_2) \le 1$, the problem (21) after applying the SDR is transformed as

$$\min_{\mathbf{S}_2 \succeq 0} \mathbf{h}_{21}^H \mathbf{S}_2 \mathbf{h}_{21} \quad (23)$$

$$s.t.\ \text{tr}(\mathbf{S}_2) \le P_2, \quad (24)$$

$$\mathbf{h}_{22}^H \mathbf{S}_2 \mathbf{h}_{22} \ge \delta, \quad (25)$$

where $\mathbf{X} \succeq 0$ indicates that a matrix $\mathbf{X}$ is positive semi-definite.

Since the problem in (23) is convex and satisfies the Slater's condition, the duality gap of (23) is zero, and thus it can be solved by the Lagrange duality method. Let us define μ and λ as the dual variables corresponding to the constraint (24) and (25), respectively. Then, it is shown in the following theorem that we can always find the rank one optimal solution $\mathbf{S}_2^\star$ for (23), and the structure of $\mathbf{S}_2^\star$ is expressed by the optimal dual solutions of the problem (23) $\mu^\star$ and $\lambda^\star$.

Theorem 2: The optimal solution for the problem (23) can be given by

$$\mathbf{S}_2^\star = q \mathbf{v} \mathbf{v}^H, \quad (26)$$

where q represents a constant with $0 \le q \le P_2$, $\mathbf{v}$ is a unit norm vector such that $\mathbf{A}\mathbf{v} = \mathbf{0}$ with $\mathbf{A} = \mathbf{h}_{21}\mathbf{h}_{21}^H + \mu^\star \mathbf{I}_M - \lambda^\star \mathbf{h}_{22}\mathbf{h}_{22}^H$, and the optimal dual variables can be either $\mu^\star = \lambda^\star = 0$ or $\mu^\star, \lambda^\star > 0$.

Proof: See Appendix A.[4] ■

Theorem 2 implies that the optimal $\mathbf{S}_2^\star$ is a rank one matrix, and thus the optimal beamforming vector $\tilde{\mathbf{w}}_2(\delta)$ can be obtained as $\tilde{\mathbf{w}}_2(\delta) = \sqrt{q}\mathbf{v}$ instead of solving the non-convex problem (21). From Theorem 2, it is easy to verify that the optimal dual variables of the problem (23), $\mu^\star$ and $\lambda^\star$, satisfy either $\mu^\star = \lambda^\star = 0$ or $\mu^\star, \lambda^\star > 0$. When the optimal dual solutions of (23) equal $\mu^\star = \lambda^\star = 0$, the matrix $\mathbf{A}$ in Theorem 2 becomes $\mathbf{A} = \mathbf{h}_{21}\mathbf{h}_{21}^H$, and this leads to $\mathbf{h}_{21}^H \mathbf{v} = 0$. This means

[3] $\tilde{\mathbf{w}}_1(\delta)$ is continuous at $\delta = Q - E_{\text{ID}}^{\text{BC}}$, and thus is also continuous at $\delta = \delta_1$.

[4] Note that the rank one property of $\mathbf{S}_2^\star$ can also be obtained from [27], but additional rank reduction algorithms are required. Moreover, it does not provide any insightful results on $\mathbf{S}_2^\star$. By examining Theorem 2, we attain important consequences for deriving a closed-form expression of $\mathbf{S}_2^\star$, which will be given in Lemma 1.

that in the case of $\mu^\star = \lambda^\star = 0$, the optimal transmission strategy at the energy transmitter is ZF for the channel $\mathbf{h}_{21}$. Therefore, by setting $q = P_2$ and $\mathbf{v} = \mathbf{\Pi}^{\perp}_{\mathbf{h}_{21}}\mathbf{h}_{22}/\|\mathbf{\Pi}^{\perp}_{\mathbf{h}_{21}}\mathbf{h}_{22}\|$, the energy transmitter can transfer the extra energy up to $E_{\mathrm{ZF}} = P_2\|\mathbf{\Pi}^{\perp}_{\mathbf{h}_{21}}\mathbf{h}_{22}\|^2$ to the EH receiver without incurring any interference to the ID receiver. Note that the case of $\mu^\star = \lambda^\star = 0$ occurs only when $\delta \le E_{\mathrm{ZF}}$, because if δ is greater than E_{ZF}, the energy transmitter cannot send energy δ to the EH receiver without interference, i.e., $I(\delta) = 0$.

Let us define the threshold δ_2 which determines the formula of $\tilde{\mathbf{w}}_2(\delta)$ as

$$\delta_2 = \begin{cases} \delta_{\min}, & \text{for } E_{\mathrm{ZF}} \le \delta_{\min} \\ \delta_{\max}, & \text{for } E_{\mathrm{ZF}} \ge \delta_{\max} \\ E_{\mathrm{ZF}}, & \text{elsewhere} \end{cases} = \max\{\delta_{\min}, E_{\mathrm{ZF}}\}, \quad (27)$$

where (27) comes from the facts that $\delta_{\max} \ge Q \ge E_{\mathrm{ID}}^{\text{IFC-PC}} > E_{\mathrm{ZF}}$. Then, for $\delta_{\min} \le \delta \le \delta_2$, a closed-form expression of the optimal beamforming vector $\tilde{\mathbf{w}}_2(\delta)$ is written by

$$\tilde{\mathbf{w}}_2(\delta) = \sqrt{P_2}\frac{\mathbf{\Pi}^{\perp}_{\mathbf{h}_{21}}\mathbf{h}_{22}}{\left\|\mathbf{\Pi}^{\perp}_{\mathbf{h}_{21}}\mathbf{h}_{22}\right\|} \triangleq \mathbf{w}_2^{\mathrm{ZF}}, \text{ for } \delta_{\min} \le \delta \le \delta_2. \quad (28)$$

On the contrary, for $\delta_2 < \delta \le \delta_{\max}$, the optimal dual solutions become positive, i.e., $\mu^\star > 0$ and $\lambda^\star > 0$. In this case, the optimal beamforming vector $\tilde{\mathbf{w}}_2(\delta)$ would be attained via existing convex optimization methods [26], but it is hard to obtain any insightful results. Instead, by reformulating the problem (23), we arrive at the following lemma which reveals a closed-form expression of $\tilde{\mathbf{w}}_2(\delta)$ for $\delta_2 < \delta \le \delta_{\max}$.

Lemma 1: For a given δ with $\delta_2 < \delta \le \delta_{\max}$, the optimal beamforming vector of the energy transmitter is given as

$$\tilde{\mathbf{w}}_2(\delta) = \sqrt{\frac{\delta}{\|\mathbf{h}_{22}\|^2}}\frac{\mathbf{h}_{22}}{\|\mathbf{h}_{22}\|} - \sqrt{P_2 - \frac{\delta}{\|\mathbf{h}_{22}\|^2}}\beta\frac{\mathbf{\Pi}^{\perp}_{\mathbf{h}_{22}}\mathbf{h}_{21}}{\left\|\mathbf{\Pi}^{\perp}_{\mathbf{h}_{22}}\mathbf{h}_{21}\right\|}, \quad (29)$$

where $\beta = \mathbf{h}_{21}^H\mathbf{h}_{22}/|\mathbf{h}_{21}^H\mathbf{h}_{22}|$.

Proof: See Appendix B.[5] ■

From (29), we can see that $\tilde{\mathbf{w}}_2(\delta)$ is expressed as a linear combination of $\mathbf{h}_{22}$ and its orthogonal complement $\mathbf{\Pi}^{\perp}_{\mathbf{h}_{22}}\mathbf{h}_{21}$. As δ grows, the energy transmitter steers its beam direction towards $\mathbf{h}_{22}$, which is the channel vector between the energy transfer and the EH receiver, to transfer more energy.

B. Optimal Energy Splitting Parameter δ

Now, based on the previous results, we can identify $\tilde{R}_{\text{IFC-PC}}(\delta, Q)$ for all feasible δ with a given Q. To obtain the Pareto boundary point, it remains to find the optimal energy splitting parameter $\delta^\star$, which requires a line search algorithm over $\delta_{\min} \le \delta \le \delta_{\max}$. The following lemma enables an efficient identification of $\delta^\star$ without loss of optimality.

Lemma 2: Let us define the received SINR at the ID receiver as $\mathrm{SINR}(\delta, Q) = \frac{P(\delta,Q)}{1+I(\delta)}$, where $P(\delta, Q) = |\mathbf{h}_{11}^H\tilde{\mathbf{w}}_1(\delta)|^2$. Then, the function $\mathrm{SINR}(\delta, Q)$ is pseudo-concave with respect to δ for a given Q.

[5] $\tilde{\mathbf{w}}_2(\delta)$ is continuous at $\delta = E_{\mathrm{ZF}}$, and thus is also continuous at $\delta = \delta_2$.

Proof: The function $\mathrm{SINR}(\delta, Q)$ is pseudo-concave, provided that $P(\delta, Q)$ is non-negative concave and $I(\delta)$ is convex on δ [28]. Since $P(\delta, Q) \ge 0$, it is sufficient to show the concavity and convexity of $P(\delta, Q)$ and $I(\delta)$, respectively. We first prove that $P(\delta, Q)$ is concave on δ. $P(\delta, Q)$ is obtained as

$$P(\delta, Q) = \begin{cases} \left(\sqrt{\frac{Q-\delta}{\|\mathbf{h}_{12}\|^2}}\frac{|\mathbf{h}_{12}^H\mathbf{h}_{11}|}{\|\mathbf{h}_{12}\|} + \sqrt{P_1 - \frac{Q-\delta}{\|\mathbf{h}_{12}\|^2}}\left\|\mathbf{\Pi}^{\perp}_{\mathbf{h}_{12}}\mathbf{h}_{11}\right\|\right)^2, & \text{for } \delta_{\min} \le \delta < \delta_1, \\ P_1\|\mathbf{h}_{11}\|^2, & \text{for } \delta_1 \le \delta \le \delta_{\max}. \end{cases}$$

One can verify that $P''(\delta, Q) < 0$ for $\delta_{\min} \le \delta < \delta_1$. Since $P(\delta, Q)$ is continuous at $\delta = \delta_1$, $P(\delta, Q)$ is a concave function for all range of δ.

Next, we consider the interference power $I(\delta) = |\mathbf{h}_{22}^H\tilde{\mathbf{w}}_2(\delta)|^2$, which is calculated as

$$I(\delta) = \begin{cases} 0, & \text{for } \delta_{\min} \le \delta \le \delta_2, \\ \left(\sqrt{\frac{\delta}{\|\mathbf{h}_{22}\|^2}}\frac{|\mathbf{h}_{21}^H\mathbf{h}_{22}|}{\|\mathbf{h}_{22}\|} - \sqrt{P_2 - \frac{\delta}{\|\mathbf{h}_{22}\|^2}}\left\|\mathbf{\Pi}^{\perp}_{\mathbf{h}_{22}}\mathbf{h}_{21}\right\|\right)^2, & \text{for } \delta_2 < \delta \le \delta_{\max}. \end{cases}$$

Similarly, we can easily check that $I(\delta)$ is convex on δ by showing that $I''(\delta) > 0$ for $\delta_2 < \delta \le \delta_{\max}$. This completes the proof. ■

Lemma 2 indicates that the function $\mathrm{SINR}(\delta, Q)$ is pseudo-concave on δ, and thereby any stationary point of $\mathrm{SINR}(\delta, Q)$ is a global maximum [28], i.e., the optimal $\delta^\star$ satisfies $\frac{\partial \mathrm{SINR}(\delta,Q)}{\partial\delta}\big|_{\delta=\delta^\star} = 0$. Since $\mathrm{SINR}(\delta, Q)$ is non-decreasing for $\delta_{\min} \le \delta \le \delta_2$ and is non-increasing for $\delta_1 \le \delta \le \delta_{\max}$, the optimal energy splitting parameter $\delta^\star$ lies in $[\delta_2, \delta_1]$.[6] Within this range, $\mathrm{SINR}(\delta, Q)$ is strictly pseudo-concave since $P''(\delta, Q) < 0$ and $I''(\delta) > 0$, and this implies that $\mathrm{SINR}(\delta, Q)$ has at most one maximum [28]. Therefore, the unique maximizer $\delta^\star$ can be efficiently found by employing the bisection method [26], [29].

The Algorithm 1 for identifying the Pareto boundary of the IFC-PC is summarized as follows:[7]

Algorithm 1 Optimal algorithm for the IFC-PC

1. Set the EH constraint $E_{\mathrm{ID}}^{\text{IFC-PC}} \le Q \le E_{\max}^{\text{IFC-PC}}$.
2. Find the optimal $\delta^\star \in [\delta_2, \delta_1]$ satisfying $\frac{\partial \mathrm{SINR}(\delta,Q)}{\partial\delta}\big|_{\delta=\delta^\star} = 0$ via the bisection method.
3. Compute the optimal beamforming vectors as $\mathbf{w}_1^\star = \tilde{\mathbf{w}}_1(\delta^\star)$ and $\mathbf{w}_2^\star = \tilde{\mathbf{w}}_2(\delta^\star)$.
4. Obtain the Pareto boundary point $(R^\star_{\text{IFC-PC}}(Q), Q)$.

V. Optimal Beamforming Vector Design for the IFC-SC

In this section, we provide the optimal transmission strategy for the IFC-SC system which achieves the Pareto boundary of the R-E region $\mathcal{C}_{\text{IFC-SC}}(P_1, P_2)$ by solving problem (5). To this end, we first introduce a power splitting parameter θ, which

[6] Since $E_{\mathrm{ID}}^{\text{IFC-PC}} \le Q \le E_{\max}^{\text{IFC-PC}}$, $\delta_2 \le \delta_1$ is always true.

[7] Without time sharing (convex hull operation), the achievable R-E region of the IFC-PC is not a convex set in general. In practice, $R^\star_{\text{IFC-PC}}(Q)$ can be computed in advance, and thus the time sharing can be employed via conventional convex hull algorithms.

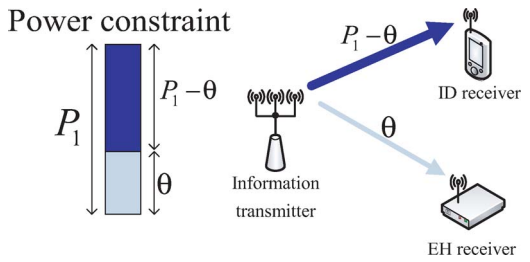

Fig. 4. Graphical interpretation of the power splitting parameter θ in the IFC-SC system.

represents the transmit power of the energy signal at the information transmitter as illustrated in Fig. 4. Then, the information transmitter allocates the power θ for the energy signal, while the remaining power $P_1-\theta$ is utilized for the information signal. The details are explained in the following subsections.

A. Characterization of the Pareto Boundary

In this subsection, we characterize the Pareto boundary of the R-E region for the IFC-SC by putting the power splitting parameter $\theta=\|\mathbf{g}_{1,\mathrm{E}}\|^2$ in the original problem (5). Denoting a unit norm vector $\mathbf{f}\in\mathbb{C}^{M\times 1}$ as $\mathbf{f}=\frac{\mathbf{g}_{1,\mathrm{E}}}{\sqrt{\theta}}$, the original problem for the IFC-SC (5) is reformulated as

$$R^{\star}_{\text{IFC-SC}}(U)=\max_{\mathbf{g}_{1,\mathrm{I}},\theta,\mathbf{f},\mathbf{g}_2}\ \log_2\left(1+\left|\mathbf{h}_{11}^H\mathbf{g}_{1,\mathrm{I}}\right|^2\right) \tag{30}$$

$$s.t.\ \|\mathbf{g}_{1,\mathrm{I}}\|^2\le P_1-\theta,\ \|\mathbf{g}_2\|^2\le P_2,\ \|\mathbf{f}\|^2=1,$$

$$\left|\mathbf{h}_{12}^H\mathbf{g}_{1,\mathrm{I}}\right|^2\ge U-\left|\mathbf{h}_{22}^H\mathbf{g}_2+\sqrt{\theta}\mathbf{h}_{12}^H\mathbf{f}\right|^2. \tag{31}$$

For a given θ, we first present the optimal solutions $\mathbf{f}^\star$ and $\mathbf{g}_2^\star$ of (30). Note that $\mathbf{f}$ and $\mathbf{g}_2$ do not affect the objective function of (30), but the feasible set of $\mathbf{g}_{1,\mathrm{I}}$, which is defined as

$$\mathcal{G}(\theta,\mathbf{f},\mathbf{g}_2)=\Big\{\mathbf{g}_{1,\mathrm{I}}:\|\mathbf{g}_{1,\mathrm{I}}\|^2\le P_1-\theta,\ \left|\mathbf{h}_{12}^H\mathbf{g}_{1,\mathrm{I}}\right|^2\ge U-\left|\mathbf{h}_{22}^H\mathbf{g}_2+\sqrt{\theta}\mathbf{h}_{12}^H\mathbf{f}\right|^2\Big\}.$$

Therefore, the optimal $\mathbf{f}^\star$ and $\mathbf{g}_2^\star$ for the problem (30) should enlarge the set $\mathcal{G}(\theta,\mathbf{f},\mathbf{g}_2)$. This leads to the following maximization problem:

$$\max_{\mathbf{f},\,\mathbf{g}_2}\left|\mathbf{h}_{22}^H\mathbf{g}_2+\sqrt{\theta}\mathbf{h}_{12}^H\mathbf{f}\right|^2,\ s.t.\ \|\mathbf{f}\|^2=1,\ \|\mathbf{g}_2\|^2\le P_2. \tag{32}$$

One can show that the objective function of (32) achieves its maximum value $\varepsilon(\theta)=(\sqrt{P_2}\|\mathbf{h}_{22}\|+\sqrt{\theta}\|\mathbf{h}_{12}\|)^2$ with the optimal solutions $\mathbf{g}_2^\star=\sqrt{P_2}\frac{\mathbf{h}_{22}}{\|\mathbf{h}_{22}\|}$ and $\mathbf{f}^\star=\frac{\mathbf{h}_{12}}{\|\mathbf{h}_{12}\|}$, i.e., both beamforming vectors are aligned to the EH receiver. Finally, the original problem (5) can be recast to

$$R^{\star}_{\text{IFC-SC}}(U)=\max_{\theta_{\min}\le\theta\le P_1}\tilde{R}_{\text{IFC-SC}}(\theta,U), \tag{33}$$

where $\theta_{\min}=\left(\frac{(U-E_{\max}^{\text{IFC-PC}})^+}{2\sqrt{P_2}\|\mathbf{h}_{12}\|\|\mathbf{h}_{22}\|}\right)^2$. Also, $\tilde{R}_{\text{IFC-SC}}(\theta,U)$ is defined as

$$\tilde{R}_{\text{IFC-SC}}(\theta,U)=\max_{\mathbf{g}_{1,\mathrm{I}}}\log_2\left(1+\left|\mathbf{h}_{11}^H\mathbf{g}_{1,\mathrm{I}}\right|^2\right)$$

$$s.t.\ \|\mathbf{g}_{1,\mathrm{I}}\|^2\le P_1-\theta,\ \left|\mathbf{h}_{12}^H\mathbf{g}_{1,\mathrm{I}}\right|^2\ge U-\varepsilon(\theta). \tag{34}$$

The proof is similar to Theorem 1, and thus is omitted for brevity. It is remarkable that in the IFC-SC systems, the Pareto boundary of the R-E region is characterized by the parameter θ, which represents the transmit power of the energy signal $\mathbf{g}_{1,\mathrm{E}}s_2$ at the information transmitter. Thus, similar to the IFC-PC scenario, the Pareto boundary point $(R^{\star}_{\text{IFC-SC}}(U),U)$ can be computed by first identifying $\tilde{R}_{\text{IFC-SC}}(\theta,U)$ for all feasible θ, and then $R^{\star}_{\text{IFC-SC}}(U)$ is obtained by searching the optimal power splitting parameter $\theta^\star$ which maximizes the information rate $\tilde{R}_{\text{IFC-SC}}(\theta,U)$ within $\theta_{\min}\le\theta\le P_1$.

B. Optimal Power Splitting Parameter θ

Now, the remaining part for finding the Pareto boundary point $(R^{\star}_{\text{IFC-SC}}(U),U)$ is solving problems (33) and (34). To this end, we first derive the optimal solution $\tilde{\mathbf{g}}_{1,\mathrm{I}}(\theta)$ for problem (34), and then prove that the optimal $\theta^\star$ can be obtained via the bisection method. Note that problem (34) is equivalent to the rate maximization problem for the BC [10]. Thus, similar to problem (22), a closed-form solution can be written by

$$\tilde{\mathbf{g}}_{1,\mathrm{I}}(\theta)=\begin{cases}\sqrt{\frac{U-\varepsilon(\theta)}{\|\mathbf{h}_{12}\|^2}}\alpha\frac{\mathbf{h}_{12}}{\|\mathbf{h}_{12}\|}\\ \quad+\sqrt{P_1-\theta-\frac{U-\varepsilon(\theta)}{\|\mathbf{h}_{12}\|^2}}\frac{\mathbf{\Pi}^{\perp}_{\mathbf{h}_{12}}\mathbf{h}_{11}}{\left\|\mathbf{\Pi}^{\perp}_{\mathbf{h}_{12}}\mathbf{h}_{11}\right\|}, & \text{for } \theta_{\min}\le\theta<\theta_1,\\ \sqrt{P_1-\theta}\frac{\mathbf{h}_{11}}{\|\mathbf{h}_{11}\|}, & \text{for } \theta_1\le\theta\le P_1,\end{cases}$$

where the threshold θ_1 is defined as $\theta_1=\min\left\{\left(\frac{\sqrt{B^2+AC}-B}{A}\right)^2,P_1\right\}$ with $A=\frac{E_{\max}^{\text{BC}}-E_{\text{ID}}^{\text{BC}}}{P_1}$, $B=\sqrt{P_2}\|\mathbf{h}_{12}\|\|\mathbf{h}_{22}\|$, and $C=U-E_{\text{ID}}^{\text{IFC-SC}}$.

Next, we present the method for identifying $\theta^\star$. By using the solution (35), $|\mathbf{h}_{11}^H\tilde{\mathbf{g}}_{1,\mathrm{I}}(\theta)|^2$ can be computed as (35), shown at the bottom of the page. One can prove that (35) is concave utilizing the fact that $\varepsilon(\theta)$ is concave, and thus $\tilde{R}_{\text{IFC-SC}}(\theta,U)$ is also concave since the logarithm is non-decreasing concave. In addition, since $\tilde{R}_{\text{IFC-SC}}(\theta,U)$ is decreasing for $\theta_1\le\theta\le P_1$, the optimal $\theta^\star$ lies in $[\theta_{\min},\theta_1]$. As a result, we can search the optimal $\theta^\star$ by applying the bisection method [26] without loss of optimality.

We summarize the method which identifies the Pareto boundary of the IFC-SC as Algorithm 2 below.

Algorithm 2 Optimal algorithm for the IFC-SC

1. Set the EH constraint $E_{\text{ID}}^{\text{IFC-SC}}\le U\le E_{\max}^{\text{IFC-SC}}$.
2. Find the optimal $\theta^\star\in[\theta_{\min},\theta_1]$ satisfying $\frac{\partial\tilde{R}_{\text{IFC-SC}}(\theta,U)}{\partial\theta}\big|_{\theta=\theta^\star}=0$ via the bisection method.
3. Compute the optimal beamforming vectors as $\mathbf{g}_{1,\mathrm{I}}^\star=\tilde{\mathbf{g}}_{1,\mathrm{I}}(\theta^\star)$, $\mathbf{g}_{1,\mathrm{E}}^\star=\sqrt{\theta^\star}\frac{\mathbf{h}_{12}}{\|\mathbf{h}_{12}\|}$, and $\mathbf{g}_2^\star=\sqrt{P_2}\frac{\mathbf{h}_{22}}{\|\mathbf{h}_{22}\|}$.
4. Obtain the Pareto boundary point $(R^{\star}_{\text{IFC-SC}}(U),U)$.

$$\left|\mathbf{h}_{11}^H\tilde{\mathbf{g}}_{1,\mathrm{I}}(\theta)\right|^2=\begin{cases}\left(\sqrt{\frac{U-\varepsilon(\theta)}{\|\mathbf{h}_{12}\|^2}}\frac{|\mathbf{h}_{12}^H\mathbf{h}_{11}|}{\|\mathbf{h}_{12}\|}+\sqrt{P_1-\theta-\frac{U-\varepsilon(\theta)}{\|\mathbf{h}_{12}\|^2}}\left\|\mathbf{\Pi}^{\perp}_{\mathbf{h}_{12}}\mathbf{h}_{11}\right\|\right)^2, & \text{for } \theta_{\min}\le\theta<\theta_1\\ (P_1-\theta)\|\mathbf{h}_{11}\|^2, & \text{for } \theta_1\le\theta\le P_1\end{cases} \tag{35}$$

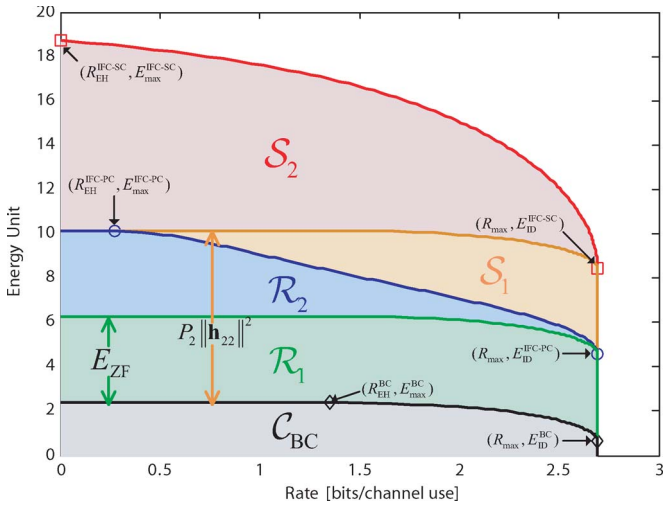

Fig. 5. Five subregions of the achievable R-E region for the IFC.

VI. Geometrical Interpretation

In this section, we geometrically describe the achievable R-E region and provide insightful observations from the results discussed in Sections III–V.

A. Transmission Strategy for Achievable R-E Region

According to value of the parameters δ and θ, we can consider five different subregions of the achievable R-E region for the IFC, which are illustrated in Fig. 5. Here, the subregion $\mathcal{C}_{\mathrm{BC}}$ stands for the achievable R-E region for the BC [10], and the boundary points are obtained with $\mathbf{w}_2 = \mathbf{0}$ in the IFC-PC. Also, the boundary points of the subregions $\mathcal{R}_1$ and $\mathcal{R}_2$ is achieved by the IFC-PC systems, while the subregions $\mathcal{S}_1$ and $\mathcal{S}_2$ can be attained by the IFC-SC protocols. In the following, we provide achievable transmission strategies for the boundary of each subregions.

1) Transmission Strategy for Boundary of $\mathcal{R}_1$: The subregion $\mathcal{R}_1$ coincides with $\delta = E_{\mathrm{ZF}}$ in the IFC-PC. Then, we can obtain the boundary points of $\mathcal{R}_1$ by employing the beamforming vectors $\mathbf{w}_1 = \tilde{\mathbf{w}}_1(E_{\mathrm{ZF}})$ and $\mathbf{w}_2 = \mathbf{w}_2^{\mathrm{ZF}}$ defined in (28). Note that when the energy transmitter employs the ZF beamforming vector $\mathbf{w}_2^{\mathrm{ZF}}$, the EH receiver harvests the additional energy E_{ZF} without interfering the ID receiver. Therefore, the region $\mathcal{R}_1$ becomes the shifted version of the BC region $\mathcal{C}_{\mathrm{BC}}$ with the enhanced energy of E_{ZF} as shown in Fig. 5.

To achieve the vertical boundary points $(R_{\max}, E)$ for $E_{\mathrm{ID}}^{\mathrm{BC}} < E < E_{\mathrm{ID}}^{\mathrm{IFC\text{-}PC}}$, we introduce a power control factor $0 < \gamma < 1$. Then, we can get the vertical boundary of the subregion $\mathcal{R}_2$ with $\mathbf{w}_1 = \mathbf{w}_1^{\mathrm{ID}}$ and $\mathbf{w}_2 = \sqrt{\gamma}\mathbf{w}_2^{\mathrm{ZF}}$ by setting the power control factor as $\gamma = (E - E_{\mathrm{ID}}^{\mathrm{BC}})/E_{\mathrm{ZF}}$. The horizontal boundary points can be computed by using the similar approach in the BC [10].

2) Transmission Strategy for Boundary of $\mathcal{R}_2$: As illustrated in Fig. 5, the region $\mathcal{R}_3$ consists of the Pareto boundary points of the IFC-PC, which are corresponding to the R-E points (R, E) for $R_{\mathrm{EH}} \le R \le R_{\max}$ and $E_{\mathrm{ID}}^{\mathrm{IFC\text{-}PC}} \le E \le E_{\max}^{\mathrm{IFC\text{-}PC}}$. As we discussed before, the boundary of $\mathcal{R}_3$ can be obtained with the energy splitting parameter $\delta^\star > E_{\mathrm{ZF}}$.

3) Transmission Strategy for Boundary of $\mathcal{S}_1$: This region corresponds to the case of $\theta = 0$ in the IFC-SC, i.e., the information transmitter does not send the energy symbol s_2. In this case, the only difference with the IFC-PC is the interference cancelling protocol at the ID receiver. Then, the energy transmitter can transfer the energy $P_2\|\mathbf{h}_{22}\|^2$ without sacrificing the maximum information rate $R_{\max}$. Thus, the subregion $\mathcal{S}_1$ becomes the shifted version of the BC region $\mathcal{C}_{\mathrm{BC}}$ with the enhanced energy of $P_2\|\mathbf{h}_{22}\|^2$ as shown in Fig. 5.

4) Transmission Strategy for Boundary of $\mathcal{S}_2$: The region $\mathcal{S}_2$ contains the Pareto boundary points of the IFC-SC. To achieve the Pareto boundary, the information transmitter should transfer both the information and the energy symbols by identifying the optimal power splitting parameter $\theta^\star > 0$.

B. Numerical Examples

In this subsection, we provide numerical examples for the Pareto boundary of the achievable R-E region and compare with conventional methods. In the simulations, ab average signal attenuation is assumed to be 60 dB for each pair of transmitter and receiver. With $M = 2$ antennas at transmitters, the channel vectors are given by

$$\mathbf{h}_{11} = 10^{-3} \times [-0.055 + 0.889j, 0.657 + 1.231j]^T,$$
$$\mathbf{h}_{12} = 10^{-3} \times [-1.081 + 1.202j, 1.298 - 1.006j]^T,$$
$$\mathbf{h}_{21} = 10^{-3} \times [-1.040 + 1.076j, -0.429 + 0.242j]^T,$$
$$\mathbf{h}_{22} = 10^{-3} \times [-0.657 + 1.299j, 0.667 + 0.296j]^T.$$

Also, we set the transmit power constraint and the noise variance as $P_1 = P_2 = 20$ dBm and -50 dBm [18], respectively.

Fig. 6(a) presents the Pareto boundary for the achievable R-E region of the IFC-PC and BC. For comparison, we also plot the achievable R-E region for the maiximum-energy (ME) beamforming [15], signal-to-leakage-and-harvested-energy ratio (SLER) maximizing beamforming [15], and the ZF beamforming[8] where the energy transmitter fixes its beamforming vector as $\mathbf{w}_2 = \mathbf{w}_2^{\mathrm{ZF}}$. It is observed that the proposed Pareto boundary for the IFC-PC generates a larger R-E region than the conventional schemes.

In Fig. 6(b), we provide the Pareto boundary of the IFC-SC and the IFC-PC systems. We can see that the achievable R-E region becomes larger when the signaling cooperation is additionally adapted in the IFC-PC.

VII. Conclusion

This paper has investigated the SWIPT system for two-user MISO IFC where one receiver decodes information and the other receiver opportunistically harvests energy from the received signal. In this configuration, we have completely characterized the Pareto boundary of the achievable R-E regions for the IFC-PC and the IFC-SC. To this end, we have constructed an information rate maximization problems with the harvested energy constraint, which are non-convex in general. To solve these non-convex problems, parameters δ and θ have been introduced for the IFC-PC and the IFC-SC, respectively. Then, the original problems for the IFC-PC and the IFC-SC are decoupled into two sequential problems, and the Pareto boundary of the

[8]Note that the minimum leakage beamforming proposed in the MIMO IFC-PC [15] becomes ZF beamforming in the MISO IFC-PC.

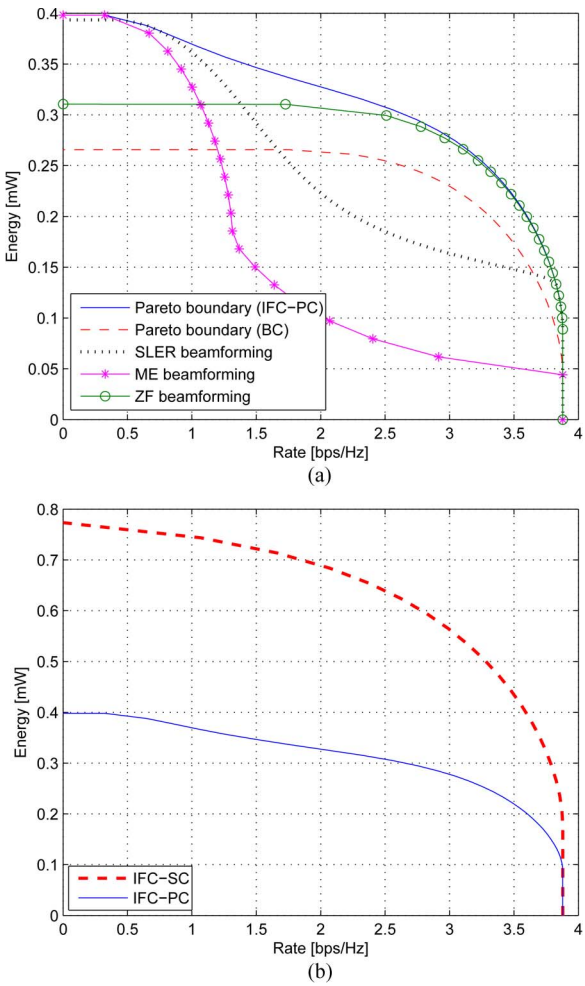

Fig. 6. The achievable R-E regions of various systems. (a) Comparison of the proposed and conventional schemes. (b) Pareto boundary for the IFC-SC and the IFC-PC.

achievable R-E regions have been identified by solving these two problems. From geometrical interpretations, we have observed insightful results on the optimal transmission strategy which achieves the Pareto boundary. Also, numerical examples have confirmed that the proposed optimal beamforming provides a lager R-E region than conventional schemes.

Appendix A
Proof of Theorem 2

The Lagrangian of (23) is formulated as

$$\mathcal{L}(\mathbf{S}_2, \mu, \lambda) = \mathrm{tr}\left(\left(\mathbf{h}_{21}\mathbf{h}_{21}^H + \mu\mathbf{I}_M - \lambda\mathbf{h}_{22}\mathbf{h}_{22}^H\right)\mathbf{S}_2\right) - \mu P_2 + \lambda\delta,$$

where μ and λ are the dual variables corresponding to the constraints (24) and (25), respectively. Let us define $\mu^\star$ and $\lambda^\star$ as the optimal dual variables of (23), and $\mathbf{A} = \mathbf{h}_{21}\mathbf{h}_{21}^H + \mu^\star\mathbf{I}_M - \lambda^\star\mathbf{h}_{22}\mathbf{h}_{22}^H$. From the Karush-Kuhn-Tucker conditions of (23), we get

$$\mathbf{A}\mathbf{S}_2^\star = \mathbf{0}, \tag{36}$$
$$\mu^\star \geq 0, \lambda^\star \geq 0, \tag{37}$$
$$\mu^\star\left(\mathrm{tr}\left(\mathbf{S}_2^\star\right) - P_2\right) = 0, \tag{38}$$
$$\lambda^\star\left(\delta - \mathbf{h}_{22}^H\mathbf{S}_2^\star\mathbf{h}_{22}\right) = 0. \tag{39}$$

Note that to ensure $\mathcal{L}(\mathbf{S}_2, \mu, \lambda) > -\infty$, $\mathbf{A}$ should satisfy $\mathbf{A} \succeq 0$.

Now, it will be shown that we can always find a rank one optimal solution for the problem (23) by using the derived optimal conditions (36)–(39) and $\mathbf{A} \succeq 0$ for the following four cases on the optimal dual variables $\mu^\star$ and $\lambda^\star$. First, we consider the case of $\mu^\star > 0$ and $\lambda^\star = 0$. In this case, $\mathbf{A}$ reduces to $\mathbf{A} = \mathbf{h}_{21}\mathbf{h}_{21}^H + \mu^\star\mathbf{I}_M$. Since $\mu^\star > 0$, we always have $\mathbf{A} \succ 0$, and thus the optimal solution for (23) is given by $\mathbf{S}_2^\star = \mathbf{0}$, which contradicts the complementary slackness condition (38).

For the second case of $\mu^\star = 0$ and $\lambda^\star > 0$, $\mathbf{A}$ becomes $\mathbf{A} = \mathbf{h}_{21}\mathbf{h}_{21}^H - \lambda^\star\mathbf{h}_{22}\mathbf{h}_{22}^H$. Note that for any non-zero vector $\mathbf{x} \in \mathbb{C}^{M\times 1}$, a positive semi-definite matrix $\mathbf{A}$ must satisfy $\mathbf{x}^H\mathbf{A}\mathbf{x} = |\mathbf{h}_{21}^H\mathbf{x}|^2 - \lambda^\star|\mathbf{h}_{22}^H\mathbf{x}|^2 \geq 0$. Then, for a non-zero vector $\mathbf{x}$ such that $\mathbf{h}_{21}^H\mathbf{x} = 0$, it follows:

$$\mathbf{x}^H\mathbf{A}\mathbf{x} = -\lambda^\star\left|\mathbf{h}_{22}^H\mathbf{x}\right|^2 \geq 0. \tag{40}$$

Since the inequality (40) is obtained only when $\lambda^\star = 0$, this contradicts the assumption $\lambda^\star > 0$.

Next, we consider the case of $\mu^\star > 0$ and $\lambda^\star > 0$ with $\mathbf{A} = \mathbf{h}_{21}\mathbf{h}_{21}^H + \mu^\star\mathbf{I}_M - \lambda^\star\mathbf{h}_{22}\mathbf{h}_{22}^H$. In this case, we will show $M - 1 \leq \mathrm{rank}(\mathbf{A}) \leq M$. It is easy to prove that for any square matrices $\mathbf{X} \in \mathbb{C}^{M\times M}$ and $\mathbf{Y} \in \mathbb{C}^{M\times M}$, the rank of $\mathbf{X} + \mathbf{Y}$ is bounded by

$$\mathrm{rank}(\mathbf{X} + \mathbf{Y}) \geq \mathrm{rank}(\mathbf{X}) - \mathrm{rank}(\mathbf{Y}). \tag{41}$$

By setting $\mathbf{X} = \mathbf{h}_{21}\mathbf{h}_{21}^H + \mu^\star\mathbf{I}$ and $\mathbf{Y} = -\lambda^\star\mathbf{h}_{22}\mathbf{h}_{22}^H$ in (41), we have $\mathrm{rank}(\mathbf{A}) \geq \mathrm{rank}(\mathbf{h}_{21}\mathbf{h}_{21}^H + \mu^\star\mathbf{I}) - \mathrm{rank}(-\lambda^\star\mathbf{h}_{22}\mathbf{h}_{22}^H) = M - 1$. Hence, the rank of $\mathbf{A}$ is bounded as $M - 1 \leq \mathrm{rank}(\mathbf{A}) \leq M$. If $\mathrm{rank}(\mathbf{A}) = M$, the optimal solution of (23) is computed as $\mathbf{S}_2^\star = \mathbf{0}$ from (36), which violates the complementary slackness conditions (38) and (39). Therefore, in this case, $\mathrm{rank}(\mathbf{A}) = M - 1$ and $\mathrm{rank}(\mathbf{S}_2^\star) = 1$ are always obtained. Due to the condition in (36), the optimal structure becomes (26).

Lastly, for $\mu^\star = \lambda^\star = 0$, $\mathbf{A}$ is written as $\mathbf{A} = \mathbf{h}_{21}\mathbf{h}_{21}^H$, and thus the optimal solution of (23) is expressed by $\mathbf{S}_2^\star = \mathbf{U}\mathbf{Q}\mathbf{U}^H$ [30], where columns of the matrix $\mathbf{U} \in \mathbb{C}^{M\times(M-1)}$ forms an orthonormal basis for the nullspace of $\mathbf{h}_{21}$ and $\mathbf{Q} \in \mathbb{C}^{(M-1)\times(M-1)}$ is a positive semi-definite matrix. In the following, we will show that a rank one solution satisfying the optimal conditions (36)–(39) can always be found. Let us denote $\mathbf{Q} = \tilde{q}\tilde{\mathbf{v}}\tilde{\mathbf{v}}^H$ where $\tilde{q}$ equals a non-negative constant and $\tilde{\mathbf{v}} \in \mathbb{C}^{(M-1)\times 1}$ indicates a unit norm vector. Then, it is easy to verify that any unit norm vector $\tilde{\mathbf{v}}$ and $\tilde{q}$ such that $\delta/|\mathbf{h}_{22}^H\mathbf{U}\tilde{\mathbf{v}}|^2 \leq \tilde{q} \leq P_2$ always satisfies the constraint (24) and (25) and the optimal conditions (36)–(39), and thus we can always find a rank one solution for (23) in the case of $\mu^\star = \lambda^\star = 0$. This completes the proof.

Appendix B
Proof of Lemma 1

Let us define singular value decomposition of the column vector $\mathbf{h}_{22}$ as

$$\mathbf{h}_{22} = \bar{\mathbf{V}}\begin{bmatrix}\|\mathbf{h}_{22}\| \\ \mathbf{0}\end{bmatrix} = \begin{bmatrix}\frac{\mathbf{h}_{22}}{\|\mathbf{h}_{22}\|} & \mathbf{V}\end{bmatrix}\begin{bmatrix}\|\mathbf{h}_{22}\| \\ \mathbf{0}\end{bmatrix}, \tag{42}$$

where the unitary matrix $\bar{\mathbf{V}} \in \mathbb{C}^{M\times M}$ contains the left singular vectors of $\mathbf{h}_{22}$, and the matrix $\mathbf{V} \in \mathbb{C}^{M\times(M-1)}$ forms an

orthogonal basis of the nullspace of $\mathbf{h}_{22}$. We also respectively represent the matrix $\bar{\mathbf{S}}_2 \in \mathbb{C}^{M\times M}$ and the vector $\bar{\mathbf{h}}_{21} \in \mathbb{C}^{M\times 1}$ as

$$\bar{\mathbf{S}}_2 = \bar{\mathbf{V}}^H \mathbf{S}_2 \bar{\mathbf{V}} \triangleq \begin{bmatrix} \sqrt{a} \\ \mathbf{b} \end{bmatrix} \begin{bmatrix} \sqrt{a} \\ \mathbf{b} \end{bmatrix}^H \text{ and } \bar{\mathbf{h}}_{21} = \bar{\mathbf{V}}^H \mathbf{h}_{21} \triangleq \begin{bmatrix} d \\ \mathbf{e} \end{bmatrix}, \quad (43)$$

where $a > 0$ and $\mathbf{b} \in \mathbb{C}^{(M-1)\times 1}$ equal the optimization variables to be determined, and we have $d = \mathbf{h}_{22}^H \mathbf{h}_{21} / \|\mathbf{h}_{22}\|^2$ and $\mathbf{e} = \mathbf{V}^H \mathbf{h}_{21}$.

Applying (42) and (43) to (23)–(25), it follows:

$$\begin{aligned} \mathbf{h}_{21}^H \mathbf{S}_2 \mathbf{h}_{21} &= \bar{\mathbf{h}}_{21}^H \bar{\mathbf{S}}_2 \bar{\mathbf{h}}_{21} = |\sqrt{a} d + \mathbf{b}^H \mathbf{e}|^2, \\ \mathrm{tr}(\mathbf{S}_2) &= \mathrm{tr}(\bar{\mathbf{S}}_2) = a + \|\mathbf{b}\|^2, \\ \mathbf{h}_{22}^H \mathbf{S}_2 \mathbf{h}_{22} &= \mathbf{h}_{22}^H \bar{\mathbf{V}} \bar{\mathbf{S}}_2 \bar{\mathbf{V}}^H \mathbf{h}_{22} = \|\mathbf{h}_{22}\|^2 a. \end{aligned}$$

Then, the problem (23) can be expressed as

$$\min_{a,\mathbf{b}} |\sqrt{a} d + \mathbf{b}^H \mathbf{e}|^2 \quad (44)$$

$$s.t.\ a + \|\mathbf{b}\|^2 \le P_2, \quad (45)$$

$$\|\mathbf{h}_{22}\|^2 a \ge \delta. \quad (46)$$

From the result of Theorem 2, for $\delta_2 < \delta \le \delta_{\max}$, the equalities in two constraints (45) and (46) always hold at the optimal point, i.e.,

$$a^\star + \|\mathbf{b}^\star\|^2 = P_2, \quad (47)$$

$$\|\mathbf{h}_{22}\|^2 a^\star = \delta, \quad (48)$$

where $a^\star$ and $\mathbf{b}^\star$ stand for the optimal solution of the problem (44). Then, by using (48), we can reformulate problem (44) as

$$\min_{\mathbf{b}} \left| \sqrt{\frac{\delta}{\|\mathbf{h}_{22}\|^2}} d + \mathbf{b}^H \mathbf{e} \right|^2, \ s.t.\ \|\mathbf{b}\|^2 = P_2 - \frac{\delta}{\|\mathbf{h}_{22}\|^2}. \quad (49)$$

Denoting ν as the dual variable corresponding to the constraint (49), the Lagrangian is given by

$$\bar{\mathcal{L}}(\mathbf{b}, \nu) = \left| \sqrt{\frac{\delta}{\|\mathbf{h}_{22}\|^2}} d + \mathbf{b}^H \mathbf{e} \right|^2 + \nu \left(\|\mathbf{b}\|^2 - P_2 + \frac{\delta}{\|\mathbf{h}_{22}\|^2} \right).$$

Setting the gradient with respect to $\mathbf{b}^H$ to zero yields

$$(\nu^\star \mathbf{I}_{M-1} + \mathbf{e}\mathbf{e}^H)\mathbf{b}^\star = -\sqrt{\frac{\delta}{\|\mathbf{h}_{22}\|^2}} d^* \mathbf{e}, \quad (50)$$

where $\nu^\star$ represents the optimal dual variable.

First, suppose that $\nu^\star = 0$. Then, it follows:

$$\frac{|\mathbf{e}^H \mathbf{b}^\star|^2}{\|\mathbf{e}\|^2} = \frac{\delta}{\|\mathbf{h}_{22}\|^2} \frac{|d|^2}{\|\mathbf{e}\|^2}.$$

Since $|\mathbf{e}^H \mathbf{b}^\star|^2 / \|\mathbf{e}\|^2$ is less than $\|\mathbf{b}^\star\|^2$, we have

$$\frac{\delta}{\|\mathbf{h}_{22}\|^2} \frac{|d|^2}{\|\mathbf{e}\|^2} < P_2 - \frac{\delta}{\|\mathbf{h}_{22}\|^2}. \quad (51)$$

However, one can show that (51) is not true for $\delta_2 < \delta \le \delta_{\max}$. Thus, $\nu^\star$ cannot be 0, and the matrix $\nu^\star \mathbf{I}_{M-1} + \mathbf{e}\mathbf{e}^H$ in (50) is always invertible.

Employing the matrix inversion lemma, $\mathbf{b}^\star$ is computed as

$$\mathbf{b}^\star = -\sqrt{\frac{\delta}{\|\mathbf{h}_{22}\|^2}} \frac{d^*}{\nu^\star + \|\mathbf{e}\|^2} \mathbf{e}. \quad (52)$$

Then, to ensure the constraint in (49), we can obtain the optimal $\nu^\star$ as

$$\nu^\star = \sqrt{\frac{\delta / \|\mathbf{h}_{22}\|}{P_2 - \delta / \|\mathbf{h}_{22}\|}} |d| \|\mathbf{e}\| - \|\mathbf{e}\|^2. \quad (53)$$

Applying (53) to (52), the optimal $\mathbf{b}^\star$ is given by

$$\mathbf{b}^\star = -\sqrt{P_2 - \frac{\delta}{\|\mathbf{h}_{22}\|^2}} \frac{d^*}{|d|} \frac{\mathbf{e}}{\|\mathbf{e}\|}.$$

Hence, the optimal beamforming vector $\tilde{\mathbf{w}}_2(\delta)$ for given $\delta_2 < \delta \le \delta_{\max}$ is expressed by

$$\begin{aligned} \tilde{\mathbf{w}}_2(\delta) &= \begin{bmatrix} \dfrac{\mathbf{h}_{22}}{\|\mathbf{h}_{22}\|} & \mathbf{V} \end{bmatrix} \begin{bmatrix} \sqrt{a^\star} \\ \mathbf{b}^\star \end{bmatrix} \\ &= \sqrt{\frac{\delta}{\|\mathbf{h}_{22}\|^2}} \frac{\mathbf{h}_{22}}{\|\mathbf{h}_{22}\|} - \sqrt{P_2 - \frac{\delta}{\|\mathbf{h}_{22}\|^2}} \beta \frac{\mathbf{\Pi}_{\mathbf{h}_{22}}^{\perp} \mathbf{h}_{21}}{\left\| \mathbf{\Pi}_{\mathbf{h}_{22}}^{\perp} \mathbf{h}_{21} \right\|}, \end{aligned}$$

where $\beta = \mathbf{h}_{21}^H \mathbf{h}_{22} / |\mathbf{h}_{21}^H \mathbf{h}_{22}|$ and $\mathbf{\Pi}_{\mathbf{h}_{22}}^{\perp} = \mathbf{V}\mathbf{V}^H$.

REFERENCES

[1] O. Ozel and S. Ulukus, "Achieving AWGN capacity under stochastic energy harvesting," *IEEE Trans. Inf. Theory*, vol. 58, no. 10, pp. 6471–6483, Oct. 2012.

[2] C. K. Ho and R. Zhang, "Optimal energy allocation for wireless communications with energy harvesting constraints," *IEEE Trans. Signal Process.*, vol. 60, no. 9, pp. 4808–4818, Sep. 2012.

[3] M. Gregori and M. Payaró, "On the precoder design of a wireless energy harvesting node in linear vector Gaussian channels with arbitrary input distribution," *IEEE Trans. Commun.*, vol. 61, no. 5, pp. 1868–1879, May 2013.

[4] C. Huang, R. Zhang, and S. Cui, "Throughput maximization for the Gaussian relay channel with energy harvesting constraints," *IEEE J. Sel. Areas Commun.*, vol. 31, no. 8, pp. 1469–1479, Aug. 2013.

[5] M. M. Tentzeris and Y. Kawahara, "Design optimization and implementation for RF energy harvesting circuits," *IEEE J. Emerging Sel. Topics Circuits Syst.*, vol. 2, no. 1, pp. 24–33, Mar. 2012.

[6] M. Pinuela, P. D. Mitcheson, and S. Lucyszyn, "Ambient RF energy harvesting in urban and semi-urban environments," *IEEE Trans. Microw. Theory Techn.*, vol. 61, no. 7, pp. 2715–2726, Jul. 2013.

[7] X. Lu, P. Wang, D. Niyato, D. I. Kim, and Z. Han, "Wireless networks with RF energy harvesting: A contemporary survey," *IEEE Commun. Surveys Tuts.*, to be published. [Online]. Available: http://arxiv.org/abs/1406.6470

[8] L. R. Varshney, "Transporting information and energy simultaneously," in *Proc. IEEE Int. Symp. Inf. Theory*, Jul. 2008, pp. 1612–1616.

[9] P. Grover and A. Sahai, "Shannon meets Tesla: Wireless information and power transfer," in *Proc. IEEE Int. Symp. Inf. Theory*, Jun. 2010, pp. 2363–2367.

[10] R. Zhang and C. K. Ho, "MIMO broadcasting for simultaneous wireless information and power transfer," *IEEE Trans. Wireless Commun.*, vol. 12, no. 5, pp. 1989–2001, May 2013.

[11] J. Xu, L. Liu, and R. Zhang, "Multiuser MISO beamforming for simultaneous wireless information and power transfer," *IEEE Trans. Signal Process.*, vol. 62, pp. 4798–4810, Sep. 2014.

[12] L. Liu, R. Zhang, and K.-C. Chua, "Secrecy wireless information and power transfer with MISO beamforming," *IEEE Trans. Signal Process.*, vol. 64, no. 7, pp. 1850–1863, Apr. 2014.

[13] A. A. Nasir, X. Zhou, S. Durrani, and R. A. Kennedy, "Relaying protocols for wireless energy harvesting and information processing," *IEEE Trans. Wireless Commun.*, vol. 12, no. 7, pp. 3622–3636, Jul. 2013.

[14] B. K. Chalise, W.-K. Ma, Y. D. Zhang, H. A. Suraweera, and M. G. Amin, "Optimum performance boundaries of OSTBC based AF-MIMO relay system with energy harvesting receiver," *IEEE Trans. Signal Process.*, vol. 61, no. 17, pp. 4199–4213, Sep. 2013.

[15] J. Park and B. Clerckx, "Joint wireless information and energy transfer in a two-user MIMO interference channel," *IEEE Trans. Wireless Commun.*, vol. 12, no. 8, pp. 4210–4221, Aug. 2013.

[16] J. Park and B. Clerckx, "Joint wireless information and energy transfer in a *K*-user MIMO interference channel," *IEEE Trans. Wireless Commun.*, vol. 13, no. 10, pp. 5781–5796, Oct. 2014.
[17] C. Shen, W.-C. Li, and T.-H. Chang, "Wireless information and energy transfer in multi-antenna interference channel," *IEEE Trans. Signal Process.*, vol. 62, no. 23, pp. 6249–6264, Dec. 2014.
[18] S. Lee, L. Liu, and R. Zhang, "Collaborative wireless energy and information transfer in interference channel," *IEEE Trans. Wireless Commun.*, vol. 14, no. 1, pp. 545–557, Jan. 2015.
[19] H. Sung, S.-H. Park, K.-J. Lee, and I. Lee, "Linear precoder designs for K-user interference channels," *IEEE Trans. Wireless Commun.*, vol. 9, no. 1, pp. 291–301, Jan. 2010.
[20] S.-H. Park, H. Park, H. Sung, and I. Lee, "Regularized transceiver designs for multi-user MIMO interference channels," *IEEE Trans. Commun.*, vol. 60, no. 9, pp. 2571–2579, Sep. 2012.
[21] S.-R. Lee, H.-B. Kong, H. Park, and I. Lee, "Beamforming designs based on an asymptotic approach in MISO interference channels," *IEEE Trans. Wireless Commun.*, vol. 12, no. 12, pp. 6430–6438, Dec. 2013.
[22] E. A. Jorswieck, E. G. Larsson, and D. Danev, "Complete characterization of the pareto boundary for the MISO interference channel," *IEEE Trans. Signal Process.*, vol. 56, no. 10, pp. 5292–5296, Oct. 2008.
[23] R. Zhang and S. Cui, "Cooperative interference management with MISO beamforming," *IEEE Trans. Signal Process.*, vol. 58, no. 10, pp. 5450–5458, Oct. 2010.
[24] J.-S. Kim, K.-J. Lee, H. Park, and I. Lee, "Transmission mode selection algorithms for spatially correlated MIMO interference channels," *IEEE Trans. Wireless Commun.*, vol. 60, no. 8, pp. 4475–4479, Aug. 2012.
[25] S.-H. Park, H. Park, and I. Lee, "Distributed beamforming techniques for weighted sum-rate maximization in MISO interference channels," *IEEE Commun. Lett.*, vol. 14, no. 12, pp. 1131–1133, Dec. 2010.
[26] S. Boyd and L. Vanderberghe, *Convex Optimization*. Cambridge, U.K.: Cambridge Univ. Press, 2004.
[27] Y. Huang and D. P. Palomar, "Rank-constrained separable semidefinite programming with applications to optimal beamforming," *IEEE Trans. Signal Process.*, vol. 58, no. 2, pp. 664–678, Feb. 2010.
[28] S. Schaible, "Fractional Programming," *Zeitschrift fur Oper. Res.*, vol. 27, no. 1, pp. 39–54, 1983.
[29] Z. Chong and E. Jorswieck, "Energy-efficient power control for MIMO time-varying channels," in *Proc. IEEE Online Conf. Green Commun.*, Sep. 2011, pp. 92–97.
[30] R. Zhang, "Cooperative multi-cell block diagonalization with per-base-station power constraints," *IEEE J. Sel. Areas Commun.*, vol. 28, no. 9, pp. 1435–1445, Dec. 2010.

Hoon Lee (S'14) received the B.S. and M.S. degrees in electrical engineering from Korea University, Seoul, Korea, in 2012 and 2014, respectively, where he is currently working toward the Ph.D. degree in the School of Electrical Engineering. During the winter of 2014, he visited Imperial College London, London, U.K., to conduct a collaborative research. His research interests include information theory and signal processing for wireless communications such as MIMO wireless network and energy harvesting communication systems.

Sang-Rim Lee (S'06) received the B.S., M.S., and Ph.D. degrees from Korea University, Seoul, Korea, in 2005, 2007, and 2013, respectively, all in electrical engineering. From 2007 to 2010, he was a Research Engineer with Samsung Electronics, where he conducted research on WiMAX systems. From 2013 to 2014, he was a Postdoctoral Fellow at Korea University. In August 2014, he joined LG Electronics, Seoul, Korea, where he is currently a Senior Research Engineer with the Advanced Standard Research and Development Laboratory. His current research interests are communication theory and signal processing techniques applied for next-generation wireless systems. He was a recipient of the Silver and Bronze Prizes in the Samsung Humantech Paper Contest in February 2012 and the Silver Prize in the Inside Edge Paper Contest held by Samsung Electro-Mechanics in 2013.

Kyoung-Jae Lee (S'06–M'11) received the B.S., M.S., and Ph.D. degrees from the School of Electrical Engineering, Korea University, Seoul, Korea, in 2005, 2007, and 2011, respectively. During the winter of 2006, he interned at Beceem Communications, Inc., Santa Clara, CA, USA, and during the summer of 2009, he visited the University of Southern California, Los Angeles, CA, as a Visiting Student. He worked as a Research Professor at Korea University in 2011. From 2011 to 2012, he was a Postdoctoral Fellow at the Wireless Networking and Communications Group, University of Texas at Austin, Austin, TX, USA. Since September 2012, he has been with the Department of Electronics and Control Engineering, Hanbat National University, Daejeon, Korea. His research interests are in communication theory, signal processing, and information theory applied to the next-generation wireless communications. He was a recipient of the Best Paper Award at IEEE VTC Fall in 2009, the IEEE ComSoc APB Outstanding Paper Award in 2013, and the IEEE ComSoc APB Outstanding Young Researcher in 2013.

Han-Bae Kong (S'09–M'15) received the B.S., M.S., and Ph.D. degrees in electrical engineering from Korea University, Seoul, Korea, in 2009, 2011, and 2015, respectively. During the winter of 2010, he visited the University of Southern California, Los Angeles, CA, USA, to conduct collaborative research. He was awarded the Bronze Prizes in the Samsung Humantech Paper Contest in February 2012 and February 2013. Since March 2015, he has been a Postdoctoral Fellow at Korea University. His research interests include information theory and signal processing for wireless communications, such as the multi-cell network, the relay network and the heterogeneous network.

Inkyu Lee (S'92–M'95–SM'01) received the B.S. (Hons.) degree in control and instrumentation engineering from Seoul National University, Seoul, Korea, in 1990 and the M.S. and Ph.D. degrees in electrical engineering from Stanford University, Stanford, CA, USA, in 1992 and 1995, respectively. From 1995 to 2001, he was a Member of Technical Staff with Bell Laboratories, Lucent Technologies, where he studied high-speed wireless system designs. From 2001 to 2002, he worked for Agere Systems (formerly Microelectronics Group of Lucent Technologies), Murray Hill, NJ, USA, as a Distinguished Member of Technical Staff. Since September 2002, he has been with Korea University, Seoul, where he is currently a Professor at the School of Electrical Engineering. During 2009, he visited the University of Southern California, Los Angeles, CA, as a Visiting Professor. He has published over 120 journal papers in IEEE and has 30 U.S. patents granted or pending. His research interests include digital communications, signal processing, and coding techniques applied for next-generation wireless systems. He has served as an Associate Editor of the IEEE TRANSACTIONS ON COMMUNICATIONS from 2001 to 2011 and IEEE TRANSACTIONS ON WIRELESS COMMUNICATIONS from 2007 to 2011. In addition, he has been a Chief Guest Editor of the IEEE JOURNAL ON SELECTED AREAS IN COMMUNICATIONS (Special Issue on 4G Wireless Systems) in 2006. He was a recipient of the IT Young Engineer Award at the IEEE/IEEK Joint Award in 2006 and of the Best Paper Award at APCC in 2006, IEEE VTC in 2009, and ISPACS in 2013. He was also a recipient of the Best Research Award from the Korea Information and Communications Society in 2011 and the Best Young Engineer Award from the National Academy of Engineering in Korea (NAEK) in 2013. He has been elected as a member of NAEK in 2015.